Geophysics Open File Report 47
Geoscience Department and
Geophysical Research Center
New Mexico Tech
Socorro, NM 87801

CRUSTAL STRUCTURE STUDY IN SOCORRO, NEW MEXICO AREA USING THE TIME-TERM METHOD

by

Douglas Carlson

Submitted in partial

fulfillment

of

the requirements

of

Geophysics 590

and the

Master's Degree Program

at

New Mexico Institue

of

Miining and Technology

December, 1983

ACKNOWLEDGEMENTS

I would like to thank the following people and institutions for their help:

Allan Sanford, my advisor, for help in interpreting the data and developing this paper, and for all the data he made available.

Larry Jaksha, from the USGS, for use of his records, as well as help in interpreting the data and in editing this paper.

Phil Carpenter, New Mexico Institue of Mining and Technology, for his aid in programming, discussions while working on the data and for help in editing this paper.

James Murdock and Allan Steepe, from the USGS, for providing the time-term program and for help in adapting the program to work on the computer system at New Mexico Institue of Mining and Technology.

Joan and Roger Carlson, my parents, for their support and encouragement over the last two years.

Los Alamos National Laboratory, the National Oceanic and Atmospheric Administration and University of Texas at El Paso for the records they provided.

ABSTRACT

In this study, the time-term method is used with Pn, P*, and Pg travel times to obtain velocity-depth models of the Socorro region of the Rio Grande rift. Stations used in this study lie within 35 km of Socorro, New Mexico, and the events used occurred between July, 1975 and September, 1983. The resulting Pg velocity is 5.76 km/sec for shots within 75 km and it is 6.25 km/sec for shots between 56-135 km. The P* velocity is 6.48 km/sec for events between 128-198 km. The Pn velocity is 8.08 km/sec for events between 193-938 km.

The thickness of Phanerozoic rocks beneath recording stations in the study area is between 0.0 and 2.5 km; the thickest sections are beneath Socorro cauldron. The Socorro cauldron deposits are thickest near the edges of the cauldron and thinnest in the middle, above an inferred resurgent dome. Crustal thickness ranges from 28.8-36.0 km for a four layer model composed of Phanerozoic rocks (3.4 km/sec), upper crust (5.76 km/sec), lower crust (6.48 km/sec) and upper mantle (8.08 km/sec). If a velocity of 6.25 km/sec is used for most of the upper crust, crustal thicknesses are increased by about 3 km from those listed above.

INTRODUCTION

The purpose of this study is to model crustal structure in the Socorro, New Mexico, area by applying the time-term method to seismic refraction data. The parameters to be determined are thickness of Phanerozoic rocks and depth to the Moho using Pg, P* and Pn arrival times. The Pg arrival is a conical seismic wave generated along the contact between Phanerozoic and Precambrian rocks, the P* arrival is a conical seismic wave generated along the Conrad discontinuity and the Pn arrival is a conical wave generated along the Moho discontinuity.

The data set includes events recorded by portable seismographs near Socorro, New Mexico, from 1975 to 1978 by the seismology group at New Mexico Institute of Mining and Technology (NMIMT), and by permanent seismographs operated by the Albuquerque Seismological Laboratory from 1976 to 1981, and jointly by USGS and NMIMT from 1982 to the present. Data from three stations in the Albuquerque Seismological Laboratory array were used in this study, while data from six stations in the USGS/NMIMT array were used. Locations of stations which were used are shown in Figure 1 and listed in Table 1. All stations with two letter designations are sites where portable units were located, three letter designations are for stations which have (had) permanent status.

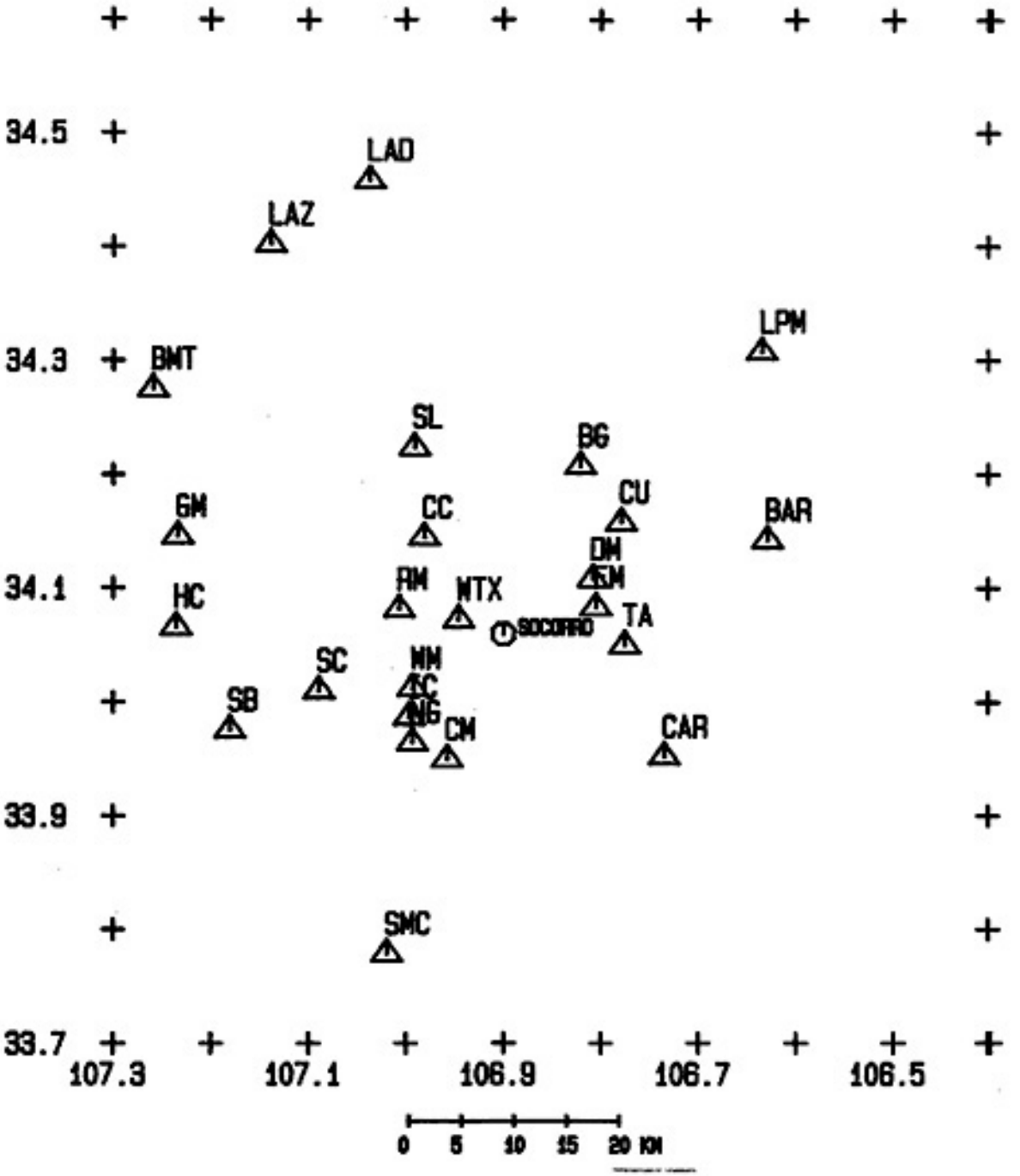

Figure 1. Seismograph stations used in this study.

TABLE 1

Stations Used For Study.

ID	Operated By	Latitude (degrees)	Longitude (degrees)	Elevation (meters)
BAR	USGS & NMT	34.1420	106.6280	2120
BG	NMT	34.2068	106.8205	1516
BMT	USGS & NMT	34.2750	107.2602	1972
CAR	USGS & NMT	33.9525	106.7345	1662
CC	NMT	34.1442	106.9819	1649
CM	NMT	33.9501	106.9576	1640
CU	NMT	34.1573	106.7785	1585
DM	NMT	34.1075	106.8079	1536
FM	NMT	34.0829	108.8047	1537
GM	NMT	34.1454	107.2345	1945
HC	NMT	34.0658	107.2361	2240
IC	NMT	33.9870	106.9967	1730
LAD	USGS & NMT	34.4583	107.0375	1768
LAZ	USGS & NMT	34.4020	107.1393	n.a.
LPM	USGS & NMT	34.3076	106.6336	1737
NG	NMT	33.9648	106.9933	1730
RM	NMT	34.0812	107.0069	1719
SB	USGS & NMT	33.9752	107.1807	3230
SC	NMT	34.0100	107.0894	2073
SL	NMT	34.2234	106.9910	1615
SMC	USGS & NMT	33.7787	107.0193	1560
SNM	NMT	34.0702	106.9435	1511
TA	NMT	34.0498	106.7751	1558
WM	NMT	34.0120	106.9929	1673
WTX	USGS & NMT	34.0722	106.9459	1555

NMT is New Mexico Institute of Mining and Technology
USGS is United States Geologic Survey

In order to use times for a given phase for a given event, that phase must be recorded at least at two stations; more stations are preferable. For Pg arrival times, explosions whose locations (and many cases origin times) were known were used. The arrivals had very clear implusive beginnings and rated 0 on a scale from 0 to 4. The seismology group at NMIMT from 1976 to 1983 timed the Pg arrivals used in this report. The P* readings represent a combination of earthquakes and explosion sources. All P* readings were implusive rating either 0 or 1 and were timed by the author. Pn readings include a mix of explosions and earthquakes as sources. For this set of data, times were read by Douglas Carlson, Larry Jaksha, and Allan Sanford. Only readings which all three labeled as implusive and for which all three times agreed to within 0.3 seconds were accepted. In fact, most arrival times agreed to within less than 0.2 seconds. This is approximately the accuracy that can be obtained with records written at 1 mm/sec. Lists of all the arrival times are given in Appendix A.

GEOLOGIC SETTING

The study area around Socorro, New Mexico, lies approximately in the center of the state and in the Rio Grande rift about 125 km south of Albuquerque. The Rio Grande rift consists of a series of north-northeast trending highly faulted en echelon structural depressions with raised margins extending from central Colorado to northern Mexico (Toppozada and Sanford, 1976). The basins making up the Rio Grande rift are from 16 to 64 km in width (Brown et al., 1980).

Three periods of large scale deformation have occurred in the area; in the late Paleozoic, late Mesozoic, and early Cenozoic. The Laramide orogeny in the early Cenozoic was the last major period of deformation before rifting took place. The rift, to a certain degree, is controlled by pre-existing structure (Cook et al., 1979).

The Rio Grande rift began to form about 30 m.y. ago (Chapin, 1979), and as it evolved, faulting occurred in two different styles. In the Oligocene to early Miocence there was rapid extension, close spaced normal faulting and strong rotation of beds (Cape et al., 1983). Mid-Miocence to Holocence crustal extension was slower with widely spaced normal faults and gentle tilting of beds (Cape et al., 1983). The inter-basin horsts formed about 9-10 m.y. ago (Sanford et al., 1977).

Volcanism occurred along the Rio Grande rift in two episodes, the first 32-20 m.y. ago and the second 5 m.y. ago to the present. Volcanism in the last 32 m.y. has occurred mainly from the middle to the west side of the rift (Brown et al., 1980). The Socorro cauldron formed about 27 m.y. ago. After the cauldron collapsed a resurgent dome formed which was separated from the walls of the cauldron by moat deposits (Chapin et al., 1978).

The rock types in the area are; Cenozoic rocks which are either terrestrial sediments or volcanics, Cretaceous marine and nonmarine sediments, Triassic and Jurassic continental deposits, Permian evaporites and terrestrial sandstones and mudstones, and Mississipian to Permian marine limestones, shale and sandstones. The average thickness of the Paleozoic and Mesozoic section is 2.8 km in the rift, while Cenozoic deposits range from 0.3-3.0 km in the rift (Cape et al., 1983). The Precambrain basement consists of metavolcanics which are intruded by granitic and gabboric plutons (Cape et al., 1983).

One feature which is rather unique in the Socorro area is the presence of an extensive mid-crustal magma body and possible small magma bodies in the upper crust. Evidence for magma bodies in the upper crust are screening of SV waves, concentration of microearthquakes, low crustal velocity and high values of Poisson's ratio (Sanford, 1978). The mid-crustal magma body covers at least 1700 km^2 and lies

at a depth of 18-20 km depth, mainly north of Socorro. It is less than one kilometer thick, is shaped like a thin sill, and may dip a few degrees to the north (Rinehart et al., 1979). The mid-crustal magma body shows no offset beneath major surface faults (Brown et al., 1979), which indicates that these faults must die out before reaching the mid-crustal magma body.

PREVIOUS RESULTS

There have been a number of different seismic crustal studies conducted in New Mexico over the last 28 years. Most of these have been conventional refraction studies, with the exception of P-wave reflection surveys by COCORP, surface wave studies by Keller et al. (1979) and spectral studies of long-period body waves by Phinney (1964). Results for the upper and lower crust are presented in Table 2. For studies conducted in the Rio Grande rift, upper crustal velocites range from 5.8-6.1 km/sec. There seems to be little control on the depth to the Conrad since values range from 18-26 km.

The COCORP study gave a velocity of 3.5 km/sec for the Phanerozoic material in the graben (Brown et al., 1979). The depths to Precambrian basement along COCORP line 1A range from 4.8 km in the basins to 1.2 km over a horst block in the middle of the rift, when using the above velocity for the Phanerozoic material (Brown et al., 1979). Below the Phanerozoic rocks, almost no reflections are present. These areas could be plutons or greatly disturbed regions. Discontinuous reflections are also present and could represent complex metamorphic terrane (Brown et al., 1979).

Ward 1980 used inversion of microearthquake data to obtain station corrections (see Figure 2). These reflect the thickness of Phanerozoic material, increase in

TABLE 2

Previous Results-Upper Crust Thickness and Velocity

Study Number	Type Of Study	Depth To Conrad (km)	Upper Crustal Velocity (km/sec)	Lower Crustal Velocity (km/Sec)	Area Of Study
1	REFRACTION	--	(5.8)	--	SW NM
2	SPECTRA OF LONG-PERIOD BODY WAVES	18-26	6.1	6.7	#ALBUQUERQUE
3	INVERSION OF MICROEARTHQUAKE DATA	--	5.83-5.87	--	#SOCORRO
4	EARTHQUAKE DATA	--	5.8	--	#SOCORRO-ALQ.
5	*REFRACTION	17.6-19.6	5.8-6.15	6.5	#CENTRAL NM
6	REFRACTION	--	(6.4)	--	NW NM
7	REFRACTION	24	6.0	6.5	W CENTRAL NM
8	*REFRACTION	--	6.16	--	CENTRAL NM

* refraction profile is shot in only one direction
( ) notes only one velocity calculated for the whole crust
study is in the Rio Grande rift at least partially

Study No.	Author(s)
1	Tatel and Tuve (1955)
2	Phinney (1964)
3	Ward, Schlue and Sanford (1981)
4	Sanford (1978)
5	Toppozada and Sanford (1976)
6	Warren and Jackson (1968)
7	Jaksha (1982)
8	Olsen et al. (1979)

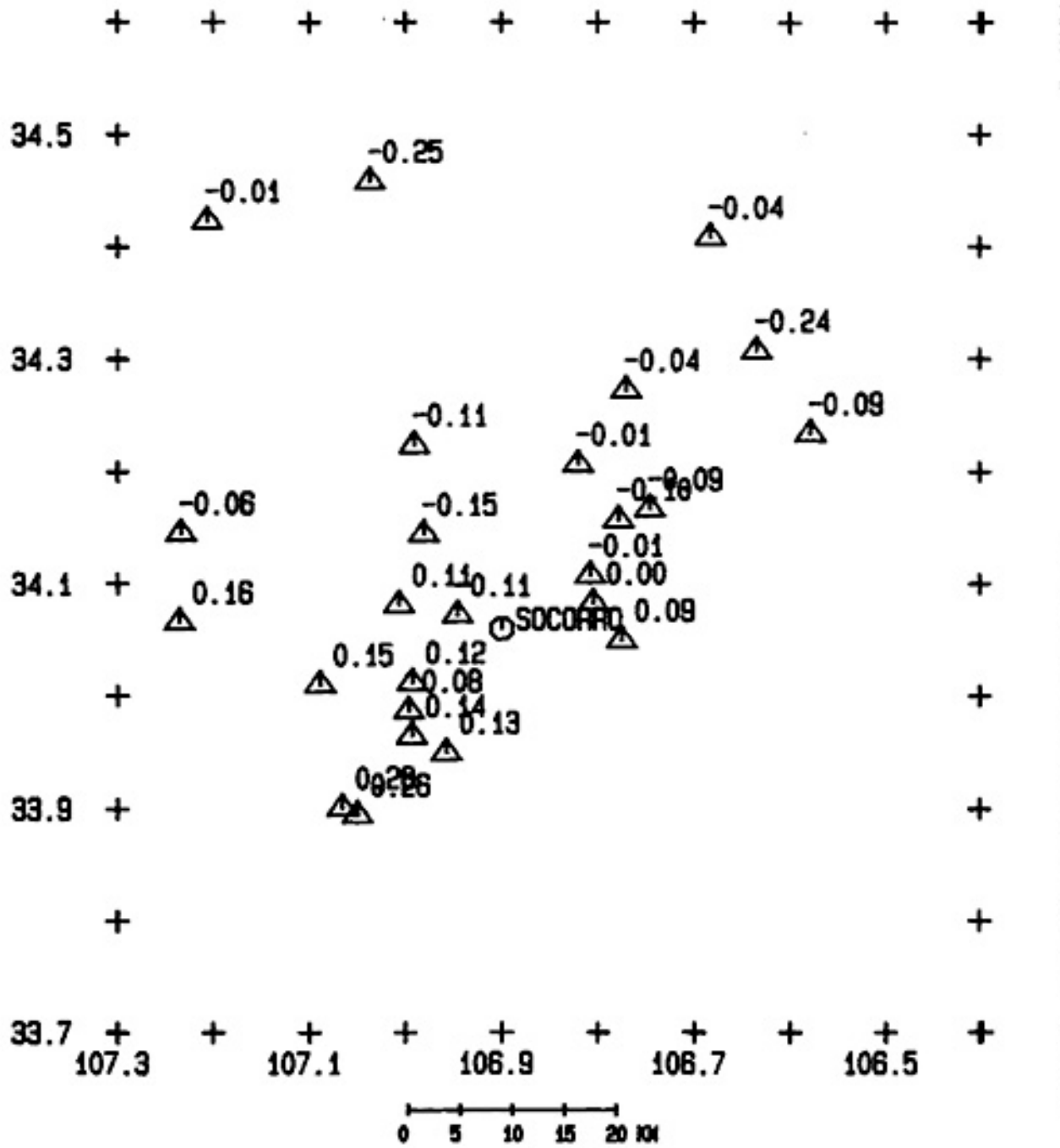

Figure 2. Station corrections as determined by Ward, (1980). All values are in seconds.

Phanerozoic rock thickness increases station correction values.

Ward et al. (1981) used inversion of microearthquake data to delineate upper crustal velocity structure near Socorro, New Mexico. The area was divided into two layers of blocks which were 0.1 degrees on an edge, the top layer of blocks being 4 km thick and the second layer being approximately 6 km thick. The resulting velocities for the upper layer of blocks ranged from 5.48-6.10 km/sec with an average velocity of 5.80 km/sec. For the lower layer, only one block had a significantly lower velocity than normal. This one block is located at the junction of the Capitan and Morenci lineaments and is a site of high earthquake activity and may contain upper crustal magma bodies (Ward et al., 1981).

Most studies have concentrated on the depth to the Moho and velocity at that boundary (see Table 3). Statewide depths to the Moho range from 27-50 km. Studies in the Rio Grande rift give depths from 27-40 km, but most of the values center around 33-35 km. Values for the uppermost mantle velocity range from 7.4-8.23 km/sec throughout the state. In the rift, values range from 7.4-8.1 km/sec with most of the values at about 7.9 km/sec. Some of the studies indicate that the Moho has a slight dip to the north along the Rio Grande rift. Toppozada and Sanford (1976) obtained a dip of 2 degrees to the north, and the surface wave study

TABLE 3

Previous Results-Depth to Moho and Pn Velocity.

Study Number	Type Of Study	Crustal Thickness (km)	Pn Velocity (km/sec)	Area Of Study
1	REFRACTION	30-35	8.1	SW NEW MEXICO
2	REFRACTION	50	8.23	E NEW MEXCIO
3	SPECTRA OF LONG-PERIOD BODY WAVES	35-40	7.4-8.4	ALBUQUERQUE
4	*REFRACTION	40	7.92	CENTRAL NEW MEXICO
5	*REFRACTION	33	7.5-7.7	CENTRAL NEW MEXICO
6	REFRACTION	27	7.4	SOUTH CENTRAL NEW MEXICO
7	**REFLECTION	33-38	--	SOCORRO
8	REFRACTION	--	8.1	CENTRAL NEW MEXICO
9	SURFACE WAVES	33-37	7.7	CENTRAL NEW MEXICO
10	REFRACTION	34.8	8.0	W NEW MEXICO
11	REFRACTION	34	--	S. RIO GRANDE RIFT
12	REFRACTION	33.3	7.9	CENTRAL NEW MEXICO
13	REFRACTION	45	7.9	NW NEW MEXICO

* refraction line was not reversed
** this is not a error bar range but indicates lateral variations

Study Number	Author(s)
1	Tatel and Tuve (1955)
2	Stewart and Pakiser (1962)
3	Phinney (1964)
4	Toppozada and Sanford (1976)
5	Olsen, Keller and Stewart (1979)
6	McCuller and Smithson (1977)
7	Brown et al. (1979)
8	Murdock and Jaksha (1978)
9	Keller, Braile and Schlue (1979)
10	Jaksha (1982)
11	Gish et al. (1981)
12	Reagor et al. (1968)
13	Warren and Jackson (1968)

by Keller et al. (1979) indicated that the Moho dips to the north along the Rio Grande rift.

A planar Moho dipping northward may be too simple a model. The COCORP study produced a range of refection travel times from 11-13 seconds for the Moho which converts to a depth range of 33-38 km along line 1A (Brown et al., 1979). It is also notable that crustal thickness under the Rio Grande rift is far less than that under the Great Plains (Toppozada ,1974).

METHOD

Computation of Velocity and Time-Terms

The time-term method was used to obtain crustal structure and velocities from refraction data for the Socorro area. This method works best when stations are deployed over an area rather than in a straight line (Reiter, 1970). The basic equation for the method is:

$$t_{ij} = a_i + a_j + \Delta_{ij}/V. \qquad (1)$$

Where t_{ij} is the theoretical travel-time, a_i the station time-term, a_j the source time-term, Δ_{ij} the distance from the station to the source and V the refractor velocity. In this formulation, velocity varies only with depth; the velocity of the halfspace is constant and the dip and/or curvature of the interfaces are small (Berry and West, 1966).

The problem is usually solved using a linear inversion scheme to obtain a model that gives the smallest least-square sum of the residuals for all the observations. The inversion gives time-terms for all sources and stations as well as the refractor velocity. These time-terms will be relative unless one station is both a receiver and a source in the data set. Another way to get absolute time-terms is to set the time-term to zero at a site where the refracting

layer outcrops (Barr, 1971).

The following discussion of the mechanics of the time-term method taken from Berry and West (1966). If there is a difference between theoretical travel-time and observed travel-time in equation (1), a residual R is left over. The residual can be expressed as

$$R_{ij} = T_{ij} - \left(\frac{\Delta_{ij}}{V} + a_i + a_2\right) , \qquad (2)$$

where T_{ij} is the observed travel-time. To simplify the equations, let $X_{ij} = T_{ij} - \Delta_{ij}/V$. Equation (2) can then be written as

$$R_{ij} = X_{ij} - a_i - a_2 . \qquad (3)$$

The maximum number of equations possible is N(N-1) where N is the number of sites. There are however, only N+1 unknowns, N time-terms and a refractor velocity. The most convenient criterion for reducing the number of equations to the number of unknowns is to require that time-terms and the refractor velocity be selected so as to minimize the sum of the squares of the residuals R_{ij} . Most data sets contain less observations than the maximum. Since not all readings exist, we need to define a new term δ_{ij} . It is 1 if an observed travel-time exists and zero if an observed travel-time does not exist. The sum of the squares of the residuals, I, can be written as

$$I = \sum_{i=1}^{N} \sum_{j=1}^{N} [x_{ij} - a_i - a_j]^2 \gamma_{ij} \quad . \qquad (4)$$

Expanding the equation and then taking its derivative I with respect to each time-term produces an equation which will give a minimum for I for each time-term

$$\frac{\partial I}{\partial a_i} = 0 = \left[a_i \sum_{j=1}^{N} \gamma_{ij} - \sum_{j=1}^{N} x_{ij} \gamma_{ij} + \sum_{j=1}^{N} a_{ij} \gamma_{ij} \right]. \qquad (5)$$

Equation (5) is just the ith equation in the set of N simultaneous linear equations. To save space the equations can be expressed in matrix notation as

$$[c_{ij}][a_{ij}] = [x_i] \quad , \qquad (6)$$

or $\quad C \times A = \bar{X}$

where $c_{ij} = \gamma_{ij}$, $i \neq j$,

$$c_{ij} = \sum_{j=1}^{N} \gamma_{ij}$$

and $\quad \bar{X}_i = \sum_{j=1}^{N} x_{ij} \gamma_{ij}$.

After formation of N normal equations, a solution can be derived by inverting the coefficient matrix C and cross mulitplying it with the data matrix X. This yields the time-term matrix A.

Now that the time-terms have been calculated, the refractor velocity can be computed. First the equation for the time-term matrix is expanded:

$$A = C^{-1} \times \bar{T} - C^{-1} \times \frac{\bar{\Delta}}{V} \quad . \qquad (7)$$

Bars over T and Δ means T and Δ are substituted in the place of $\bar{x}$ in the expression above. The value of the rth time-term can be written as

$$a_r = e_r - \frac{f_r}{V} \qquad (8)$$

where e_r is an element of $C^{-1} \times \bar{T}$. If the number of data are significantly larger than number of unknowns, it is possible to calculate the least-squares refractor velocity. We start out with equation (4) and fill in the appropriate values for the time terms

$$I = \sum_{j=1}^{N} \sum_{i=1}^{N} \left[T_{ij} - \frac{\Delta_{ij}}{V} - e_i - \frac{f_i}{V} - e_j - \frac{f_j}{V} \right]^2 \gamma_{ij} . \qquad (9)$$

Next expand equation (9), differentiate with respect to 1/V, collect terms and equate the results to zero to obtain the least-square velocity

$$V = \frac{\sum_{j=1}^{N} \sum_{i=1}^{N} \left[\Delta_{ij} - f_i - f_j \right]^2 \gamma_{ij}}{\sum_{j=1}^{N} \sum_{i=1}^{N} \left[\Delta_{ij} - f_i - f_j \right] \left[T_{ij} - e_j - e_i \right] \gamma_{ij}} \quad . \qquad (10)$$

Error Analysis

Because we are dealing with real data, there are a number of sources of error. Errors can arise in reading arrival-times, calculating origin times and locations and in misidentifying refracted waves. The following is a brief discussion on uncertainties in the method that result from errors in the data (Murdock and Jaksha, 1980). The most important measure of the fit of the model is the standard deviation of the solution which is given by the equation below.

$$S^2 = \frac{\sum_{i=1}^{N}\sum_{j=1}^{N} R_{ij}^2 \gamma_{ij}}{\sum_{i=1}^{N}\sum_{j=1}^{N} \gamma_{ij} - 2(N+1)} . \qquad (11)$$

This is a more conservative equation than Berry and West (1966) use because N is replaced with 2(N+1). We do use the Berry and West (1966) formulation for standard deviation of time-terms $\bar{\sigma}_t$ as follows

$$\bar{\sigma}_t = \frac{\sum_{s=1}^{N} R_{st}^2 \gamma_{st}}{\sum_{s=1}^{N} \gamma_{st} - 1} . \qquad (12)$$

It is important to realize that the standard deviation is a reflection of goodness of fit and it does not necessarily indicate accuracy.

Draper and Smith (1966) have a method for estimating uncertainties by employing straightfoward multiple linear regression. From this point on, Draper and Smith (1966) notation is used. The basic equation for multiple linear regression is:

$$X'X\,B = X'Y \qquad (13)$$

X is coefficient matrix, B is vector of the time-terms and 1/V parameters Y is vector of travel-times. The coefficient matrix rows are zero except for a 1 at each station and source pair. Next, solve for the parameters

$$B = (X'X)^{-1}X'Y \qquad (14)$$

The first N rows are time-terms while for the last row is 1/V. $(X'X)\delta^2$ is called the variance-covariance matrix. If the time-term model is correct, then $S = \delta^2$ (the true variance). The estimate of the ith parameter's standard error is $s\sqrt{c_{ii}}$ where c_{ii} is a principal diagonal element of the (X'X) matrix as noted in Draper and Smith (1966). The sum of the square of (s) of the residuals is

$$S = YY' - B'X'Y \qquad (15)$$

The mean square about the regression is

$$S^2 = \frac{S}{L-(N+1)} \qquad (16)$$

where L-(N+1) is the number of degrees of freedom.

With the uncertainty formulation described above, we can determine how errors influence the results. One of the great advantages of the time-term method is that uncertainties in origin-time and distance are almost entirely absorbed into the event time-terms (McCollom and Crosson, 1975). This feature is particularly useful in this study since the only time-terms of interest are the station time-terms near Socorro, New Mexico. If timing errors are consistent for either a station or source site, the error will be absorbed into the the source time-term, otherwise random errors show up in residuals (Willmore and Bancroft, 1960). Another positive point of the time-term method is that an error in velocity will mainly affect the time-terms of sources rather than the station time-terms (Murdock and Jaksha, 1980). Generally, stations that lie on the edge of the array are prone to greater errors in time-terms than stations in the interior of an array. There are several ways to reduce errors in a time-term study: (1) Increase the number of readings at each site, and (2) Bracket the stations as much as possible with events from a number of different azimuths (Willmore and Bancroft, 1960). If the events have a wide azimuthal distribution, the effect of

high-dip angles will be minimized. Even if azimuthal distribution of events is not wide, results will probably not be impaired too badly by dips under 10 degrees; for example, calculated depths are about three percent too small for a refractor with a dip of seven degrees (Reiter, 1970). Calculated depths will also be too small if there is an anticline under the array (Reiter, 1970).

In summary, if events have a fairly wide azimuthal distribution, and if the number of readings is significantly greater than unknowns, and structures have gentle dips (under 10 degrees), the time-term method will give accurate results.

RESULTS

This section presents the data and the results of the time-term analysis. The arrival first studied was Pg. This is the conical wave which travels along the interface between Phanerozoic and Precambrian rock. All the events used for the Pg study were explosions. Explosions have the advantage that their locations and origin times are usually known. Two Pg data sets were used, one for sources within 75 km of the stations and the other for sources 56 to 135 km from the stations (see Figure 3 for locations of sources in both data sets). The list of TERA and San Marcial explosions used for this study (events within 75 km) is given in Table 4. TERA and San Marcial events had an implusive Pg arrival at four or more stations. Figure 4 and Table 5 give the time terms for Pg arrival times from near-by explosions (< 75 km). The estimated velocity is 5.76±0.05 km/sec and time-terms range from -0.4 to 0.62 seconds. The uncertainties shown for the velocities in Tables 3-17 are one standard deviation.

The velocity for Pg waves is significantly higher when using explosions at 56-135 km than when using explosions at distances less than 75 km. The results from this data set are listed in Table 7 and the distribution of time-terms is shown in Figure 5. The velocity is 6.25±0.08 km/sec, while the time-terms range from 0.04 to 0.76 seconds. The 56 to

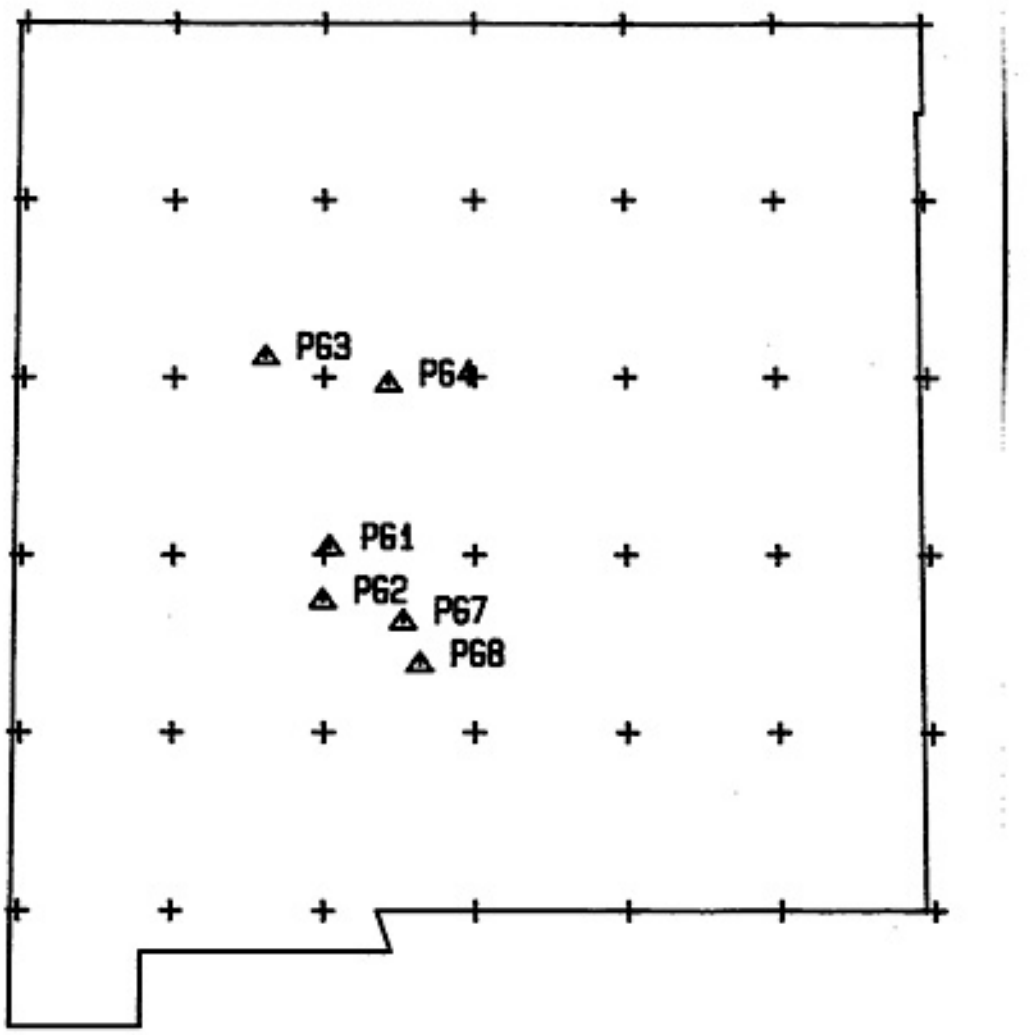

Figure 3. Location of events used in the Pg studies. PG1 represents TERA explosions at 34.039 N and 106.963 W. PG2 represents San Marcial explosions at 33.74 N and 107.01 W. PG8(White Sands Missile Range) represents PGF9 listed in Table 6, PG4 (Kirtland Air Force Base) represents PGF4 and PGF7 in Table 6, PG7(White Sands Missle Range) represents PGF1, PGF2, PGF8 in Table 6 and PG3(Jackpile Mine) represents PGF5, PGF3 and PGF6.

TABLE 4

List of Near-By Explosions Used to Calculate Pg Velocity and Time-Terms.

ID	Latitude (degrees)	Longitude (degrees)	Date (month/day/year)	Origin Time (hour:min:sec)
PGS1	34.039	106.963	7/23/75	16:51:51.04
PGS2	34.039	106.963	4/20/76	18:56:12.44
PGS3	34.039	106.963	4/21/76	19:16:43.59
PGS4	34.039	106.963	4/22/76	19:45:27.45
PGS5	34.039	106.963	2/22/77	18:47:53.88
PGS6	34.039	106.963	2/23/77	18:48:58.48
PGS7	34.039	106.963	5/10/77	23:48:24.69
PGS8	34.039	106.963	5/11/77	20:43:25.92
PGS9	34.042	106.961	5/14/77	19:50:28.56
PGS10	34.042	106.961	5/19/77	22:49:51.48
PGS11	34.039	106.963	12/ 6/77	19:47:57.45
PGS12	34.039	106.963	12/ 7/77	23:23:23.54
PGS13	34.041	106.963	9/21/82	22:42:14.23
PGS14	34.041	106.963	10/ 4 82	20:51:40.93
PGS15	33.739	107.010	10/18/82	18:06:40.33
PGS16	33.739	107.010	11/16/82	00:14:22.23
PGS17	33.739	107.010	11/18/82	00:05:22.93
PGS18	33.739	107.010	1/ 9/83	23:46:45.13
PGS19	33.739	107.010	1/26/83	23:41:27.07
PGS20	33.739	107.010	2/ 6/83	23:48:24.63
PGS21	34.041	106.963	7/21/83	18:51:20.33

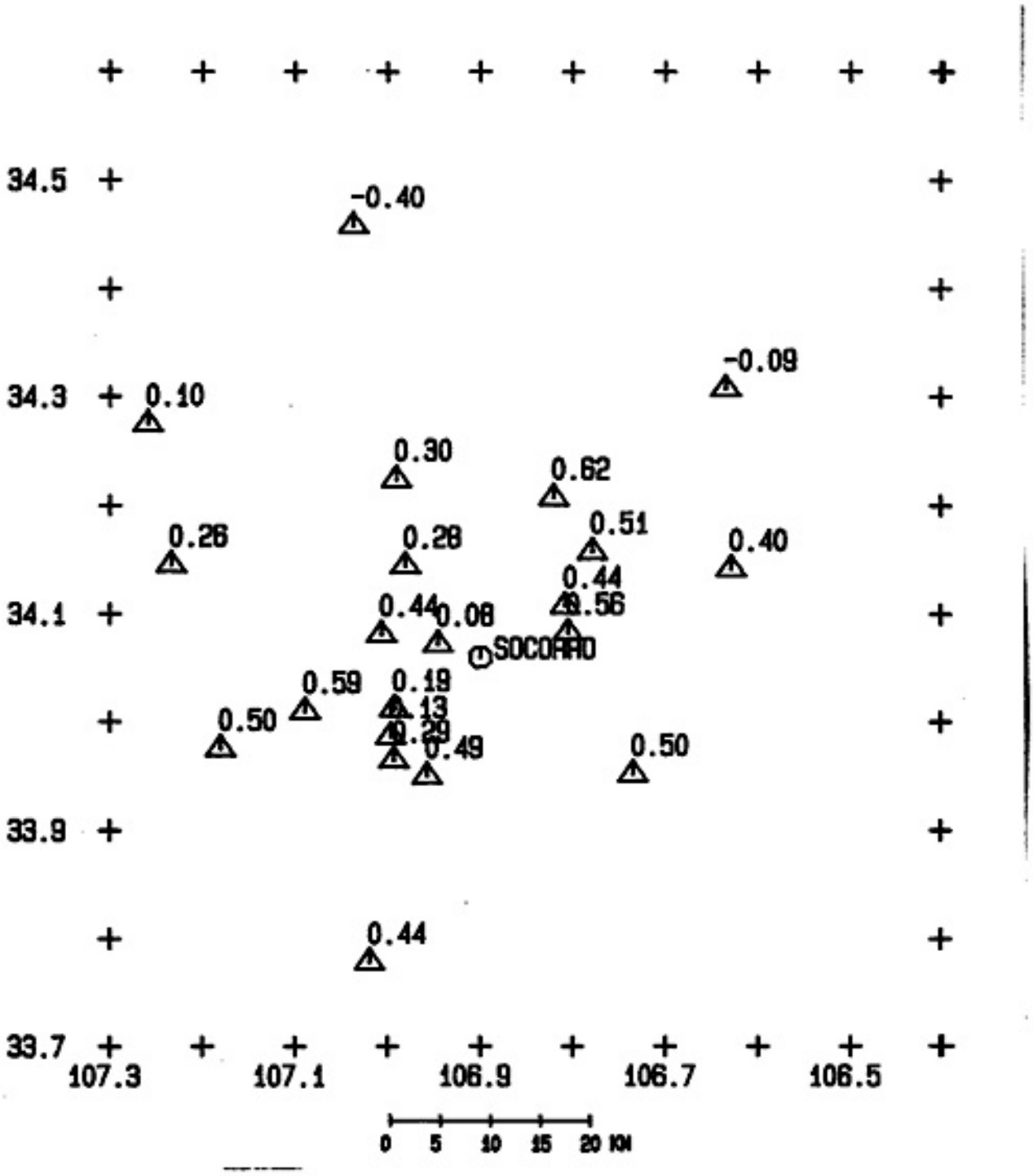

Figure 4. Pg time-terms based on shots within 75 km of the stations. All values are in seconds.

TABLE 5

Pg Velocity And Associated Time-Terms from Explosions at Distances Less Than 75 kilometers.

Velocity 5.76 km/sec and Standard Deviation of Velocity is 0.05 km/sec.
Standard Deviation of Solution is 0.09 seconds.
There are 56 Degrees of Freedom.

Site ID	Time-Term (seconds)	Standard Error (seconds)	Mean Residual (seconds)	Number Of Data
SMC	0.44	0.07	0.04	7
WTX	0.08	0.05	0.04	16
BAR	0.40	0.07	0.07	8
BMT	0.10	0.08	0.06	6
LPM	-0.09	0.08	0.07	6
SB	0.50	0.07	0.07	7
CAR	0.50	0.07	0.11	5
CC	0.28	0.08	0.05	8
SC	0.59	0.09	0.04	3
FM	0.56	0.08	0.02	4
DM	0.44	0.08	0.02	5
SL	0.30	0.08	0.04	5
BG	0.62	0.09	0.01	4
CU	0.51	0.10	0.04	2
GM	0.26	0.13	0.00	1
IC	0.13	0.10	0.01	2
NG	0.29	0.13	0.00	1
CM	0.49	0.10	0.03	2
RM	0.44	0.13	0.00	1
LAD	-0.40	0.12	0.00	2
WM	0.19	0.13	0.00	1
PGS1	0.22	0.09	0.03	3
PGS2	0.47	0.07	0.04	6
PGS3	0.44	0.07	0.04	6
PGS4	0.44	0.07	0.04	4
PGS5	0.44	0.08	0.02	5
PGS6	0.37	0.09	0.04	4
PGS7	0.50	0.09	0.01	5
PGS8	0.46	0.09	0.00	3
PGS9	0.12	0.09	0.02	2
PGS10	0.13	0.08	0.01	3
PGS11	0.34	0.07	0.02	5
PGS12	0.35	0.08	0.01	4
PGS13	0.32	0.07	0.15	4
PGS14	0.12	0.07	0.03	7
PGS15	0.62	0.08	0.10	5
PGS16	0.46	0.08	0.05	5
PGS17	0.56	0.08	0.07	6
PGS18	0.54	0.09	0.06	3
PGS19	0.53	0.08	0.05	6
PGS20	0.46	0.08	0.08	6
PGS21	0.13	0.07	0.06	5

TABLE 6

List of Distant Explosions Used to Calculate Pg Velocity and Associated Time-Terms.

ID	Latitude (degrees)	Longitude (degrees)	Date (month/day/year)	Origin Time (hour:min.:sec)
PGF1	33.788	106.365	8/12/75	17:00:00.00
PGF2	33.679	106.521	10/ 6/76	14:00:00.50
PGF3	35.111	107.393	2/14/77	23:31:43.80
PGF4	34.960	106.574	6/ 2/77	19:59:59.73
PGF5	35.111	107.393	7/27/77	22:29:15.65
PGF6	35.111	107.393	8/25/77	19:57:24.15
PGF7	34.960	106.580	6/ 8/81	16:44:59.48
PGF8	33.621	106.477	9/16/81	12:35:39.07
PGF9	33.381	106.367	10/ 7/81	16:59:59.87

TABLE 7

Pg Velocity and Associated Time-Terms from Explosions at Distances from 56 to 135 kilometers.

Velocity 6.25 km/sec and Standard Deviation of Velocity is 0.08 km/sec
Standard Deviation of Solution is 0.17 Seconds.
There are 27 Degrees of Freedom.

Site ID	Time-Term (seconds)	Standard Error (seconds)	Mean Residual (seconds)	Number Of Data
SNM	0.37	0.15	0.16	3
LPM	0.04	0.11	0.15	8
LAD	0.31	0.13	0.10	7
DM	0.38	0.15	0.05	3
IC	0.55	0.17	0.08	2
WTX	0.49	0.11	0.11	6
SC	0.76	0.14	0.16	4
CM	0.44	0.18	0.09	2
CC	0.36	0.14	0.07	5
GM	0.51	0.15	0.08	4
BG	0.67	0.17	0.04	2
PGF1	0.11	0.20	0.11	4
PGF2	0.14	0.15	0.13	7
PGF3	0.15	0.24	0.06	6
PGF4	0.15	0.19	0.16	5
PGF5	0.11	0.21	0.09	5
PGF6	0.13	0.22	0.15	8
PGF7	0.16	0.19	0.04	2
PGF8	0.11	0.18	0.07	5
PGF9	0.17	0.22	0.09	4

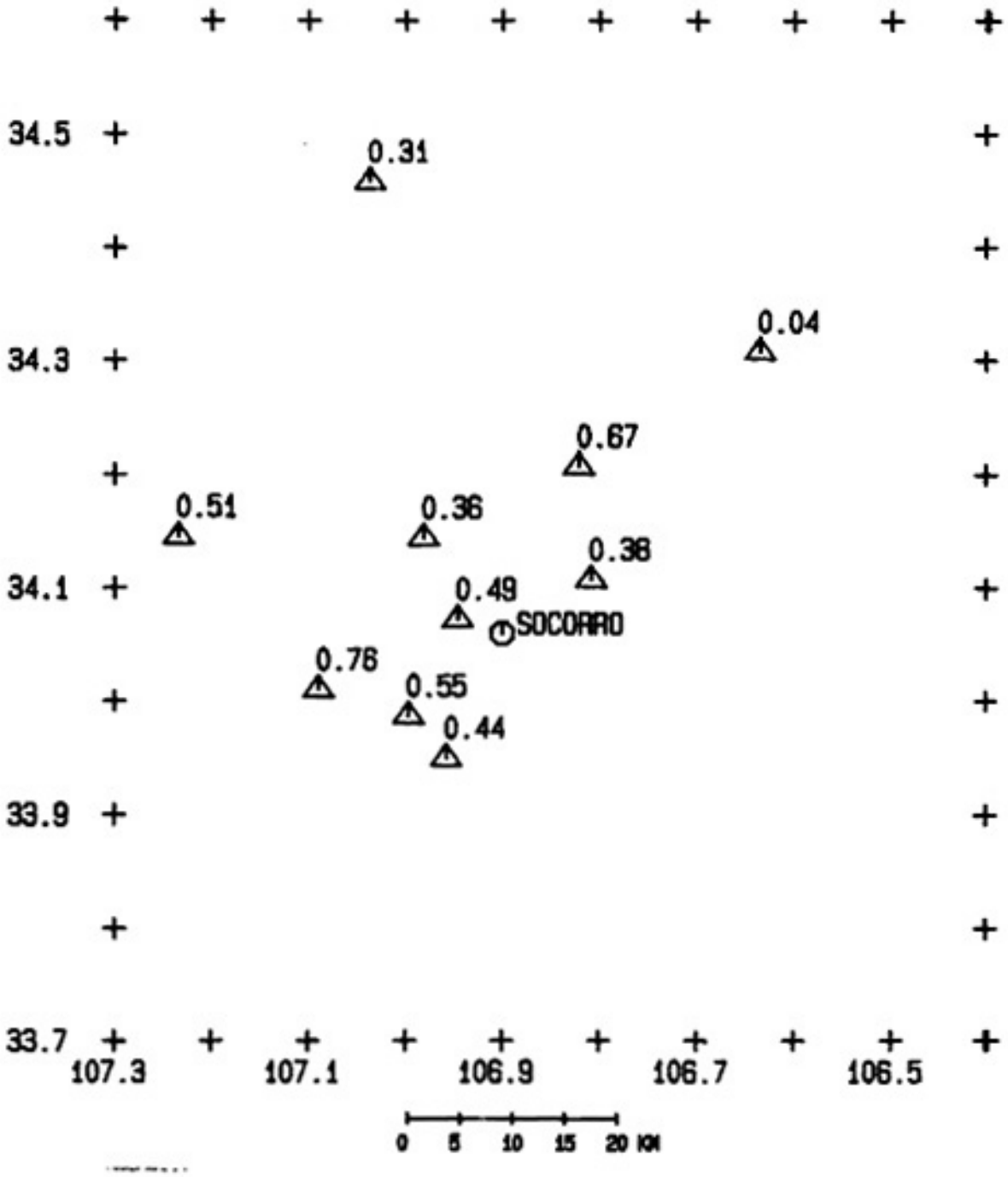

Figure 5. Pg time-terms based on events that are between 56 and 135 km from the stations. All values are in seconds.

135 km data set shows some inconsistenties. In Table 7, the time-term for WTX is greater than for PGF2, a shot at Kirtland Air Force Base. This is a problem since WTX lies on Precambrian rock while the Kirtland Air Force Base shot lies over thousands of meters of Cenozoic fill. This result can be explained by the fact the velocity model is dominated by shots from White Sands Missile Range, and the other sources will be forced to have time-terms which are not reasonable in order to minimize residuals for the whole data set.

The next arrival studied was P* which is a conical wave traveling along the Conrad discontinuity. Figure 6 and Table 8 give the location of the events used in the study of P*. This is the only data set in which the time-terms are not absolute. The Pg study produced absolute time-terms since the approximately zero value of the LPM time-term fits with the fact that Precambrian rock outcrops at the station. The Pn study produced time-terms relative to the absolute time-terms LPM and WTX which are used as an imaginary source-station pair with the refractor velocity found by Murdock and Jaksha (1980). This is the necessary tie for the data set. P* is a first arrival over only a narrow range of distances. For example, in an area with an upper crustal velocity of 5.8 km/sec and a lower crustal velocity of 6.5 km/sec, the range is about 130-190 km for a surface explosion. The scarcity and weakness of P* arrivals leads to larger uncertainties than for the Pg arrivals. Resulting

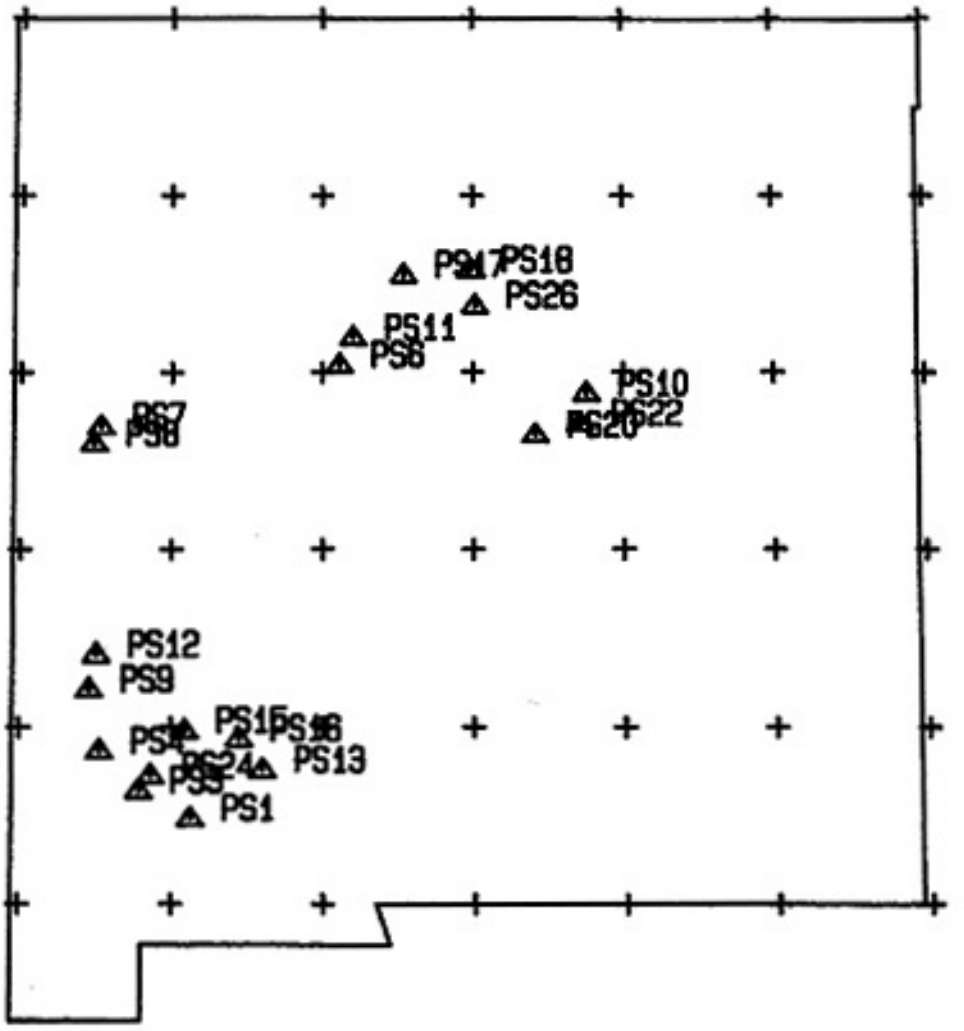

Figure 6. Events used in the P* set of data. The following symbols on this map represent more than one event: PS1 also represents PS2; PS3 also represents PS5 and PS25; PS13 also represents PS14; PS18 also represents PS19 and PS21; and PS22 also represents PS23.

TABLE 8

List of Explosions and Earthquakes Used Which Have P* Readings.

ID	Latitude (degrees)	Longitude (degrees)	Date (month/day/year)	Origin time (hour:min.:sec.)
PS1	32.478	107.872	6/16/76	18:58:51.49
PS2	32.490	107.828	7/15/76	18:56:28.66
PS3	32.637	108.212	8/ 5/76	19:49:59.81
PS4	32.861	108.472	8/23/76	19:10:56.19
PS5	32.640	108.056	9/ 1/76	20:18:20.81
PS6	35.038	106.887	10/ 8/76	15:44:50.80
PS7	34.688	108.470	4/ 7/77	11:58:50.71
PS8	34.592	108.516	4/12/77	12:16:52.03
PS9	33.207	108.542	4/26/77	20:43:56.97
PS10	34.874	105.245	7/21/78	05:02:37.70
PS11	35.193	106.797	3/30/79	10:41:55.80
PS12	33.403	108.495	5/25/82	21:44:14.63
PS13	32.754	107.395	6/ 1/82	21:34:04.43
PS14	32.713	107.397	6/ 3/82	21:26:47.84
PS15	32.976	107.911	6/ 7/82	21:28:04.73
PS16	32.930	107.553	6/22/82	01:06:44.34
PS17	35.548	106.460	9/ 8/82	23:05:33.83
PS18	35.576	106.017	9/17/82	22:33:15.54
PS19	35.433	106.111	10/19/82	23:13:31.83
PS20	34.638	105.585	1/17/83	18:58:54.63
PS21	35.408	106.118	2/11/83	20:45:01.16
PS22	34.706	105.290	5/27/83	22:27:31.69
PS23	34.740	105.338	6/16/83	22:52:27.69
PS24	32.720	108.133	8/10/83	20:01:58.43
PS25	32.689	108.241	8/12/83	20:21:31.28
PS26	35.374	105.985	9/13/83	00:01:08.48

TABLE 9

P* Velocity and Associated Time-Terms

Velocity 6.48 km/sec and Standard Deviation of Velocity is 0.14 km/sec.
Standard Deviation of Solution is 0.32 Seconds.
Number of Degrees of Freedom is 25.

Site ID	Time-Term (seconds)	Standard Error (seconds)	Mean Residual (seconds)	Number Of Data
WTX	2.15	0.19	0.14	8
SB	3.07	0.26	0.12	4
LPM	1.84	0.21	0.17	10
CAR	2.47	0.26	0.09	7
BAR	1.73	0.27	0.19	6
SMC	3.11	0.42	0.02	2
LAZ	3.02	0.36	0.07	3
NG	1.77	0.72	0.05	3
SC	1.78	0.67	0.28	7
RM	1.97	0.73	0.24	2
GM	2.19	0.64	0.22	6
HC	2.17	0.71	0.16	2
CC	1.78	0.64	0.09	3
LAD	2.33	0.49	0.00	2
PS1	-0.67	1.00	0.21	3
PS2	-0.62	1.00	0.17	3
PS3	-0.97	1.01	0.06	2
PS4	-1.13	0.98	0.21	3
PS5	-1.03	0.98	0.22	3
PS6	-1.46	0.82	0.38	2
PS7	-1.19	0.86	0.32	3
PS8	-1.24	0.86	0.09	3
PS9	-3.11	0.87	0.01	3
PS10	-1.29	0.67	0.00	2
PS11	-1.41	0.43	0.34	2
PS12	-1.82	0.57	0.16	3
PS13	-1.34	0.58	0.08	2
PS14	-1.28	0.60	0.03	2
PS15	-1.76	0.59	0.34	2
PS16	-1.04	0.54	0.06	2
PS17	-0.78	0.60	0.22	2
PS18	-1.11	0.64	0.00	2
PS19	-1.39	0.52	0.34	2
PS20	-0.48	0.51	0.02	2
PS21	-0.24	0.51	0.21	2
PS22	-1.70	0.51	0.08	2
PS23	-1.76	0.51	0.09	6
PS24	-2.07	0.62	0.15	3
PS25	-1.85	0.65	0.01	3
PS26	-0.80	0.58	0.19	2

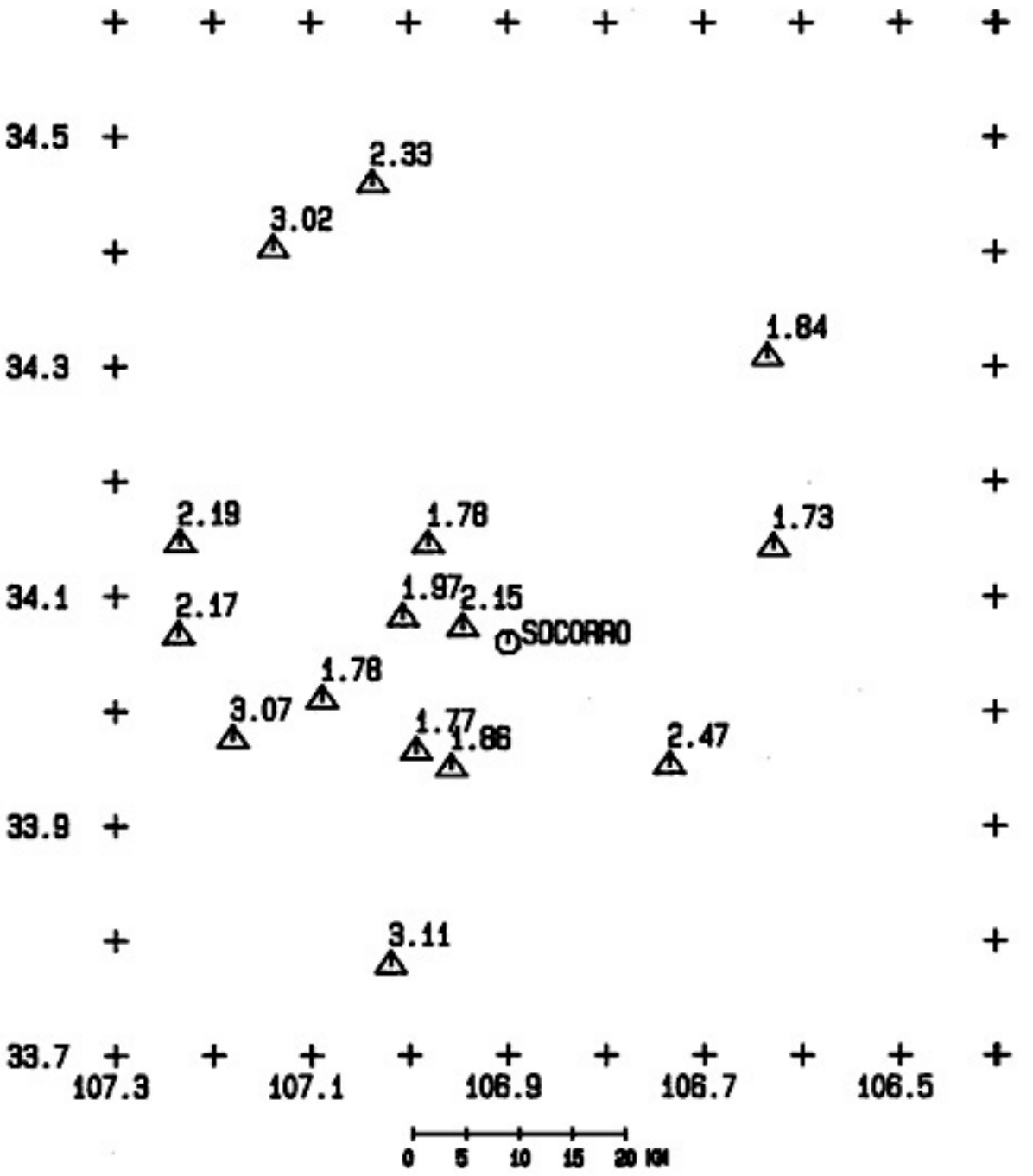

Figure 7. P* time-terms. All values are in seconds. These are only relative time-terms.

time-terms and velocities are given in Table 9 and Figure 7. The velocity is 6.48±0.14 km/sec and the relative time terms range from 1.77 to 3.02 seconds.

The most extensive study conducted was on the Pn data set. Figure 8 displays the location of the epicenters. For complete information on origin times and locations of all events used in the Pn study, see Table 10 and Figure 8. Results obtained when using all the data are presented in Figure 9 and Table 11. The velocity is 8.08±0.17 km/sec and the time-terms for the stations range from 3.47-4.14 seconds. To study the stability of the results, a number of data sets with certain lower or upper bounds for travel distance were also used (Tables 12 to 19). Most of the data sets gave velocities that agreed with the velocity when all the data was used, except those which limited readings of events to within 400 and 300 km of Socorro, respectively (Tables 15 and 16). These events give sub-Moho velocities of 7.68±0.53 km/sec and 7.67±0.64 km/sec and the time-terms have values that are about 0.4 seconds lower than those in the complete set of data.

The low velocities shown in Tables 15 and 16 are not significant. The one sigma velocity uncertainties overlap with the uncertainties for the higher velocity value, 8.08 km/sec, which is from the complete set of data. The increase in uncertainties for data sets given in Tables 15 and 16 is due to a poorer azimuthal distribution of events

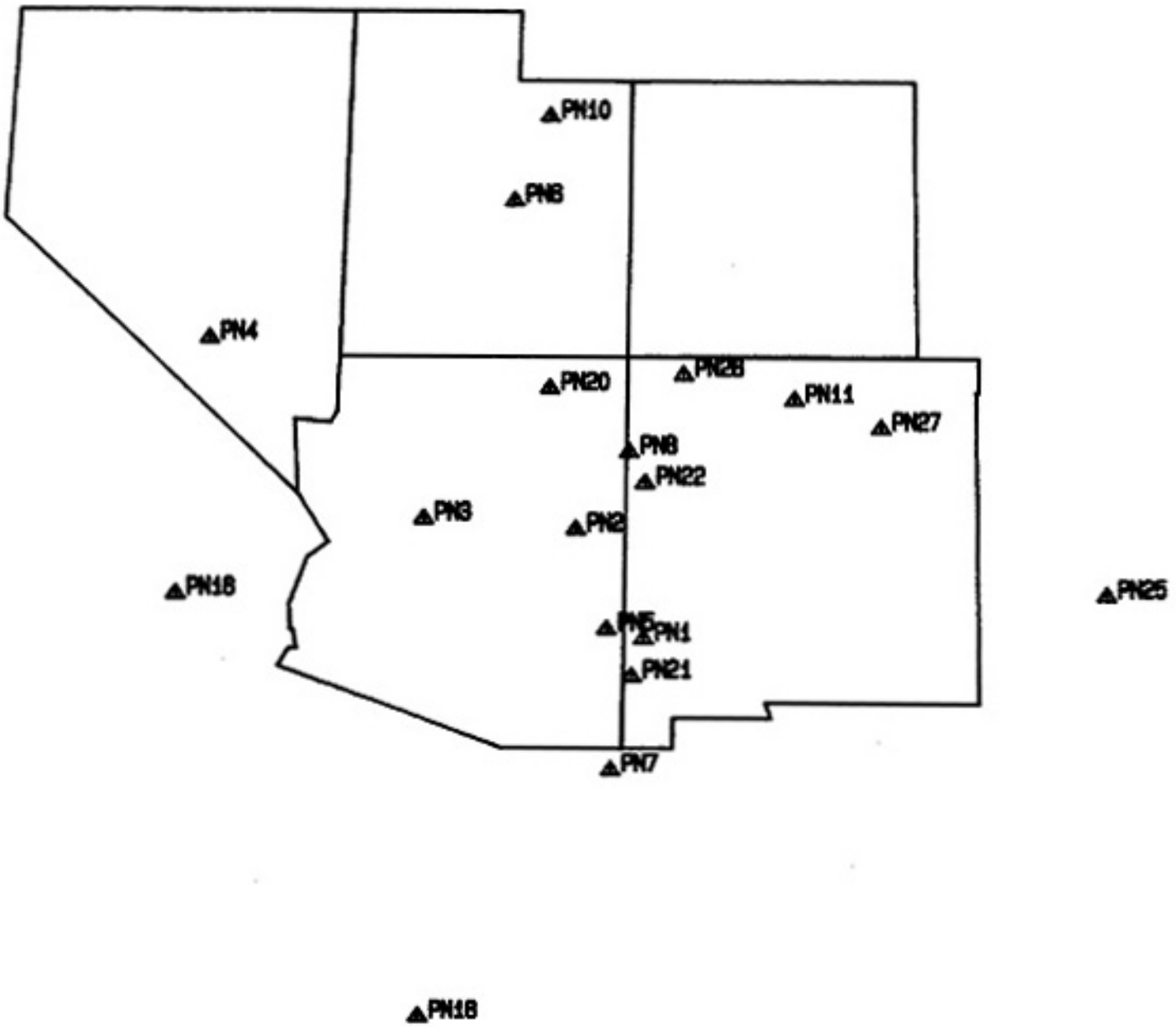

Figure 8. Events used in Pn time-term study. Some of the symbols in the figure represent more than one event: PN4 also represents PN17; PN20 also represents PN24; PN21 also represents PN12, PN13, PN14, PN15 and PN23; PN8 also represents PN9; and PN5 also represents PN19.

TABLE 10

Events Used In Pn Time-Term Study

ID	Latitude (degrees)	Longitude (degrees)	Date (month/day/year)	Origin Time (hour:min.:sec.)
PN1	32.919	108.710	1/29/76	08:04:28.46
PN2	34.507	109.891	1/30/76	08:45:01.55
PN3	34.655	112.500	2/ 4/76	00:04:58.10
PN4	37.256	116.312	3/17/76	14:15:00.10
PN5	33.063	109.335	8/ 4/76	22:31:35.44
PN6	39.272	111.080	8/19/76	13:29:53.30
PN7	31.024	109.227	6/ 8/77	13:09:07.40
PN8	35.627	109.000	7/20/77	07:40:49.49
PN9	35.627	109.000	9/23/77	14:03:00.50
PN10	40.490	110.490	10/11/77	07:56:06.50
PN11	36.377	106.174	3/ 5/79	13:00:02.70
PN12	32.270	108.760	5/ 3/81	22:54:11.58
PN13	32.289	108.970	5/ 4/81	10:55:32.32
PN14	32.242	108.926	5/ 7/81	01:38:20.22
PN15	32.280	108.920	5/11/81	23:28:13.08
PN16	33.550	116.667	6/15/82	23:49:21.30
PN17	37.236	116.370	6/24/82	14:15:00.00
PN18	27.421	112.332	7/11/82	18:02:22.30
PN19	33.063	109.335	10/21/82	22:31:53.82
PN20	36.540	110.386	10/23/82	20:14:37.06
PN21	32.378	108.900	10/28/82	12:13:22.40
PN22	35.175	108.722	11/ 3/82	17:54:11.57
PN23	32.281	108.749	11/ 5/82	11:58:22.08
PN24	36.540	110.386	11/21/82	00:53:30.22
PN25	33.578	100.871	11/28/82	02:36:49.19
PN26	36.741	108.083	2/17/83	20:50:26.21
PN27	35.974	104.676	6/30/83	02:12:18.53

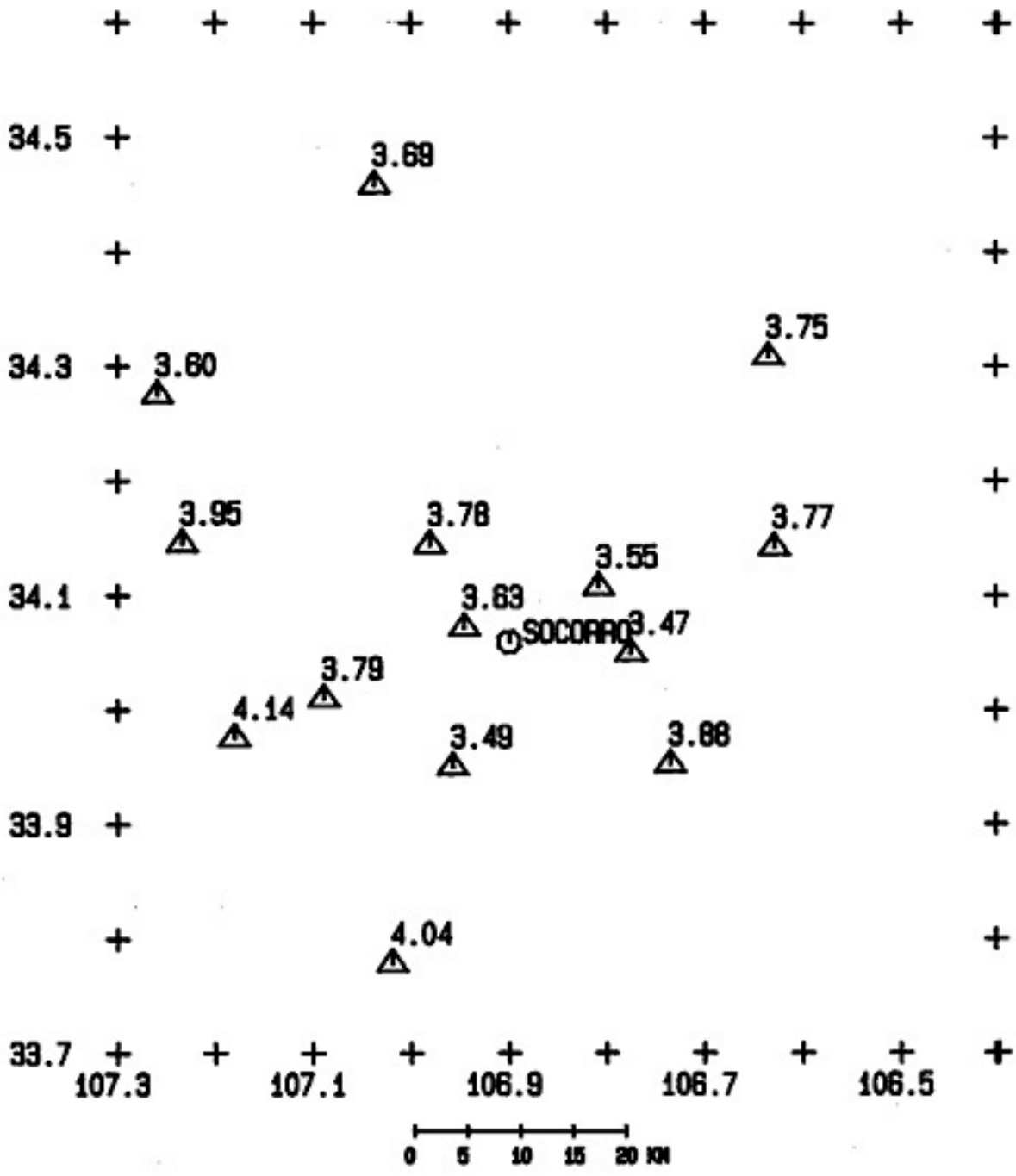

Figure 9. Pn time-terms when all events are used. All values are in seconds.

TABLE 11

Pn Velocity and Associated Time-Terms Using All Pn Readings

Velocity 8.08 km/sec and Standard Deviation of Velocity is 0.17 km/sec.
Standard Deviation of Solution is 0.26 Seconds.
Number of Degrees of Freedom is 41.

Site ID	Time-Term (seconds)	Standard Error (seconds)	Mean Residual (seconds)	Number Of Data
DM	3.55	0.21	0.13	5
SC	3.79	0.21	0.08	5
CC	3.78	0.22	0.17	5
WTX	3.63	0.15	0.12	12
TA	3.47	0.25	0.18	3
CM	3.49	0.26	0.08	3
LPM	3.75	0.16	0.12	15
LAD	3.69	0.19	0.08	7
GM	3.95	0.26	0.05	3
BMT	3.60	0.18	0.17	8
SB	4.14	0.24	0.16	3
BAR	3.77	0.22	0.14	4
CAR	3.88	0.22	0.20	5
SMC	4.04	0.24	0.39	3
PN1	2.45	0.55	0.18	5
PN2	2.16	0.72	0.16	4
PN3	4.44	1.32	0.13	6
PN4	5.63	2.35	0.11	4
PN5	3.10	0.67	0.05	2
PN6	5.63	1.78	0.05	2
PN7	4.43	1.05	0.09	5
PN8	1.81	0.66	0.01	3
PN9	4.70	0.69	0.08	2
PN10	2.89	1.94	0.09	3
PN11	5.57	0.60	0.04	2
PN12	0.92	0.77	0.12	2
PN13	1.51	0.79	0.05	2
PN14	2.03	0.79	0.03	2
PN15	1.87	0.78	0.03	2
PN16	3.22	2.31	0.16	3
PN17	5.64	2.32	0.02	3
PN18	2.36	2.34	0.14	3
PN19	2.31	0.71	0.11	3
PN20	3.08	1.03	0.26	6
PN21	1.41	0.67	0.19	2
PN22	0.90	0.57	0.16	5
PN23	1.95	0.69	0.02	2
PN24	0.36	1.02	0.23	2
PN25	6.63	1.43	0.44	4
PN26	3.53	0.80	0.24	2
PN27	4.17	0.71	0.12	2

TABLE 12

Pn Velocity and Associated Time-Terms Using Pn Readings for Events Within 700 km of the Stations

Velocity 8.04 km/sec and Standard Deviation of Velocity is 0.21 km/sec.
Standard Deviation of Solution is 0.28 Seconds.
Number of Degrees of Freedom is 30,

Site ID	Time-Term (seconds)	Standard Error (seconds)	Mean Residual (seconds)	Number Of Data
DM	3.53	0.25	0.13	4
SC	3.79	0.23	0.08	5
CC	3.73	0.25	0.18	5
WTX	3.70	0.17	0.10	7
TA	3.36	0.31	0.19	2
CM	3.33	0.34	0.03	2
LPM	3.66	0.19	0.12	12
LAD	3.66	0.22	0.07	6
GM	3.94	0.28	0.06	3
BMT	3.42	0.24	0.18	6
BAR	3.70	0.25	0.13	4
CAR	3.78	0.25	0.22	5
SMC	3.93	0.27	0.38	3
SB	4.02	0.32	0.28	2
PN1	2.33	0.69	0.15	5
PN2	2.06	0.91	0.14	4
PN3	4.13	1.17	0.16	6
PN5	2.90	0.84	0.02	2
PN6	5.19	2.25	0.06	2
PN7	4.17	1.32	0.08	5
PN8	1.75	0.82	0.02	3
PN9	4.57	0.84	0.09	2
PN11	5.48	0.74	0.01	2
PN12	0.79	0.94	0.15	2
PN13	1.37	0.97	0.02	2
PN14	1.90	0.98	0.01	2
PN15	1.74	0.96	0.06	2
PN19	2.16	0.88	0.08	3
PN20	2.90	1.27	0.21	6
PN21	1.39	0.80	0.21	2
PN22	0.81	0.69	0.19	5
PN23	1.91	0.83	0.05	2
PN24	0.23	1.26	0.18	2
PN25	6.38	1.78	0.43	4
PN26	3.48	0.96	0.29	2
PN27	4.07	0.87	0.13	2

TABLE 13

Pn Velocity and Associated Time-Terms Using Pn Readings for Events Within 600 km of the Stations

Velocity 8.03 km/sec and Standard Deviation of Velocity is 0.21 km/sec.
Standard Deviation of Solution is 0.29 Seconds.
Number of Degrees of Freedom is 29.

Site ID	Time-Term (seconds)	Standard Error (seconds)	Mean Residual (seconds)	Number Of Data
DM	3.52	0.25	0.13	4
SC	3.81	0.23	0.08	4
CC	3.73	0.25	0.17	5
WTX	3.70	0.17	0.10	7
TA	3.36	0.32	0.19	2
CM	3.32	0.35	0.03	2
LPM	3.65	0.19	0.13	12
LAD	3.66	0.22	0.07	6
GM	3.90	0.31	0.07	2
BAR	3.70	0.26	0.13	4
SB	4.02	0.32	0.29	2
CAR	3.77	0.26	0.22	5
BMT	3.42	0.25	0.18	6
SMC	3.93	0.28	0.38	3
PN1	2.30	0.70	0.15	5
PN2	2.02	0.93	0.14	4
PN3	4.05	1.70	0.16	6
PN5	2.85	0.86	0.02	2
PN7	4.12	1.34	0.09	5
PN8	1.72	0.83	0.02	3
PN9	4.56	0.86	0.07	2
PN11	5.45	0.75	0.01	2
PN12	0.74	0.96	0.15	2
PN13	1.33	0.99	0.02	2
PN14	1.85	1.00	0.00	2
PN15	1.70	1.00	0.06	2
PN19	2.12	0.90	0.08	3
PN20	2.84	1.30	0.21	6
PN21	1.35	0.81	0.21	2
PN22	0.78	0.71	0.19	5
PN23	1.87	0.85	0.05	2
PN24	0.17	1.29	0.17	2
PN25	6.30	1.82	0.42	4
PN26	3.43	0.98	0.29	2
PN27	4.03	0.89	0.13	2

TABLE 14

Pn Velocity and Associated Time-Terms Using Pn Readings for Events Within 500 km of the Stations

Velocity 7.98 km/sec and Standard Deviation of Velocity is 0.27 km/sec.
Standard Deviation of Solution is 0.22 Seconds.
Number of Degrees of Freedom is 21.

Site ID	Time-Term (seconds)	Standard Error (seconds)	Mean Residual (seconds)	Number Of Data
DM	3.49	0.23	0.10	3
SC	3.90	0.21	0.07	3
CC	3.83	0.24	0.17	4
WTX	3.70	0.14	0.11	6
TA	3.39	0.27	0.19	2
CM	3.39	0.31	0.04	2
LPM	3.62	0.19	0.07	10
GM	3.96	0.26	0.04	2
LAD	3.57	0.22	0.06	5
BAR	3.57	0.22	0.12	4
SB	3.94	0.26	0.28	2
CAR	3.55	0.25	0.19	4
BMT	3.37	0.20	0.11	5
SMC	3.42	0.25	0.03	2
PN1	2.08	0.86	0.14	5
PN2	1.74	1.14	0.17	4
PN5	2.60	1.05	0.06	2
PN7	3.76	1.66	0.06	5
PN8	1.44	1.00	0.03	3
PN9	4.27	1.03	0.04	2
PN11	5.31	0.87	0.05	2
PN12	0.55	1.14	0.12	2
PN13	1.13	1.18	0.05	2
PN14	1.65	1.19	0.04	2
PN15	1.50	1.17	0.02	2
PN19	1.93	1.09	0.04	3
PN20	2.57	1.62	0.19	6
PN21	1.42	1.03	0.03	2
PN22	0.76	0.87	0.12	5
PN23	1.78	1.04	0.03	2
PN24	-0.13	1.60	0.15	2
PN26	3.24	1.23	0.28	2
PN27	3.96	1.06	0.17	2

TABLE 15

Pn Velocity and Associated Time-Terms Using Pn Readings for Events Within 400 km of the Stations

Velocity 7.68 km/sec and Standard Deviation of Velocity is 0.53 km/sec.
Standard Deviation of Solution is 0.18 Seconds.
Number of Degrees of Freedom is 12.

Site ID	Time-Term (seconds)	Standard Error (seconds)	Mean Residual (seconds)	Number Of Data
DM	3.24	0.31	0.13	2
SC	3.74	0.23	0.01	3
CC	3.62	0.25	0.16	4
WTX	3.58	0.15	0.08	4
TA	3.12	0.32	0.17	2
CM	3.14	0.31	0.02	2
GM	3.72	0.28	0.01	2
LPM	3.56	0.29	0.05	7
LAD	3.55	0.25	0.06	5
BAR	3.49	0.31	0.10	3
BMT	3.26	0.49	0.06	2
SMC	3.38	0.34	0.06	2
CAR	3.61	0.44	0.04	3
PN1	1.28	1.70	0.12	5
PN2	0.64	2.24	0.15	4
PN5	1.56	2.10	0.01	2
PN7	2.16	3.36	0.01	2
PN8	0.52	1.94	0.02	2
PN9	3.36	2.02	0.01	2
PN11	4.25	1.74	0.04	2
PN12	-0.82	2.29	0.12	2
PN13	-0.29	2.38	0.06	2
PN14	0.22	2.39	0.04	2
PN15	0.09	2.36	0.02	2
PN19	0.67	2.20	0.09	3
PN21	0.32	1.77	0.06	2
PN22	-0.27	1.68	0.08	5
PN23	0.56	1.83	0.06	2
PN27	2.63	2.07	0.05	2

TABLE 16

Pn Velocity and Associated Time-Terms Using Pn Readings for Events Within 300 km of the Stations

Velocity 7.67 km/sec and Standard Deviation of Velocity is 0.64 km/sec.
Standard Deviation of Solution is 0.22 Seconds.
Number of Degrees of Freedom is 7.

Site ID	Time-Term (seconds)	Standard Error (seconds)	Mean Residual (seconds)	Number Of Data
DM	3.24	0.38	0.13	2
SC	3.74	0.28	0.01	2
CC	3.63	0.32	0.20	3
WTX	3.58	0.18	0.08	4
TA	3.12	0.40	0.17	2
CM	3.14	0.39	0.02	2
LPM	3.55	0.37	0.04	2
BAR	3.48	0.39	0.09	3
BMT	3.25	0.62	0.06	2
SMC	3.37	0.42	0.06	2
CAR	3.59	0.55	0.04	3
PN1	1.22	2.16	0.12	5
PN2	0.56	2.86	0.15	4
PN5	1.49	2.66	0.01	2
PN8	0.45	2.48	0.02	2
PN19	0.60	2.79	0.09	3
PN21	0.26	2.25	0.06	2
PN22	-0.32	2.14	0.08	5
PN23	0.50	2.33	0.06	2
PN27	2.57	2.63	0.04	2

TABLE 17

Pn Velocity and Associated Time-Terms Using Pn Readings for Events Farther than 300 km from the Stations

Velocity 8.13 km/sec and Standard Deviation of Velocity is 0.21 km/sec.
Standard Deviation of Solution is 0.27 Seconds.
Number of Degrees of Freedom is 18.

Site ID	Time-Term (seconds)	Standard Error (seconds)	Mean Residual (seconds)	Number Of Data
SC	3.83	0.25	0.12	3
WTX	3.65	0.16	0.15	8
DM	3.63	0.24	0.07	3
LPM	3.77	0.17	0.12	10
LAD	3.72	0.22	0.09	4
GM	4.03	0.30	0.02	2
BMT	3.56	0.19	0.14	6
SB	4.31	0.27	0.12	2
CAR	3.91	0.27	0.44	2
PN3	4.85	1.58	0.08	6
PN4	6.18	2.82	0.01	2
PN6	6.09	2.13	0.02	2
PN7	4.70	1.25	0.09	5
PN10	3.50	2.33	0.11	3
PN13	1.73	0.94	0.04	2
PN14	2.25	0.95	0.03	2
PN16	3.93	2.76	0.17	3
PN17	6.30	2.79	0.08	3
PN18	3.08	2.80	0.16	3
PN20	3.34	1.23	0.24	5
PN24	6.77	1.22	0.22	2
PN25	6.87	1.71	0.30	3

TABLE 18

Pn Velocity and Associated Time-Terms Using Pn Readings for Events Beyond 400 km from the Stations

Velocity 8.25 km/sec and Standard Deviation of Velocity is 0.25 km/sec.
Standard Deviation of Solution is 0.29 Seconds.
Number of Degrees of Freedom is 12.

Site ID	Time-Term (seconds)	Standard Error (seconds)	Mean Residual (seconds)	Number Of Data
WTX	3.68	0.17	0.16	8
DM	3.66	0.27	0.04	3
LPM	3.81	0.19	0.11	8
LAD	3.62	0.29	0.13	2
BMT	3.71	0.24	0.05	4
SB	4.34	0.29	0.08	2
CAR	3.95	0.30	0.45	2
PN3	5.79	1.93	0.10	4
PN4	7.76	3.43	0.02	2
PN7	5.34	1.52	0.04	3
PN10	4.83	2.84	0.08	3
PN16	5.42	3.34	0.14	3
PN17	7.80	3.38	0.06	3
PN18	4.60	3.39	0.15	3
PN20	4.06	1.52	0.27	4
PN25	7.78	2.07	0.29	3

TABLE 19

Pn Velocity and Associated Time-Terms Using Pn Readings for Events Beyond 500 km from the Stations

Velocity 7.95 km/sec and Standard Deviation of Velocity is 0.10 km/sec.
Standard Deviation of Solution is 0.11 Seconds.
Number of Degrees of Freedom is 7.

Site ID	Time-Term (seconds)	Standard Error (seconds)	Mean Residual (seconds)	Number Of Data
WTX	3.52	0.07	0.06	6
DM	3.57	0.12	0.04	2
LPM	3.79	0.08	0.05	5
LAD	3.67	0.11	0.11	2
BMT	3.75	0.09	0.06	4
PN3	3.44	0.84	0.07	4
PN4	3.61	1.48	0.04	2
PN10	1.35	1.23	0.07	3
PN16	1.29	1.45	0.08	3
PN17	3.71	1.46	0.07	2
PN18	4.06	1.47	0.04	3
PN25	4.90	0.91	0.03	2

than for the complete set. The loss of PN25, PN20 and PN7 cause the azimuthal range to decrease when you cut out events beyond 400 km, which is done in data sets given in Tables 15 and 16. This reduction of azimuthal range for data in Tables 15 and 16 is a violation of the assumption that there exists a wide azimuthal distribution of events (Reiter, 1970).

Table 20 summarizies the velocities and time-terms from Tables 11 to 19. It can be seen that velocity and station time-terms only change in a minor way while the event time-terms change greatly. This behavior was noted by McCollon and Crosson (1975).

The final question addressed is that of overlap of the data sets for the different refractors and whether this will cause errors. To see how many readings for different data sets fall into the overlap zones between data sets, see Table 21. Overlap zones are ranges of distances in which two different refractor arrivals are recorded. The vast majority of readings for each data set lie outside the overlap regions. 89% to 100% of all events are dominated by readings outside of overlap zones for each data set (see Table 22). Dominated means an event has 50% or more of its readings from a given distance range. The results in Tables 5,7,9 and 11 also indicate that readings in overlap zones have little or no influence on results; if they did, the one sigma uncertainties for each refractor would be far

TABLE 20

Summary Of Results For Pn Data

Table No.	11	12	13	14	15	16	17	18	19
Mean Vel. (Km/Sec)	8.08	8.04	8.03	7.98	7.68	7.67	8.13	8.25	7.95
S.D.S (Seconds)	0.26	0.28	0.29	0.22	0.18	0.22	0.27	0.29	0.11
N.D.F.	41	30	29	21	12	7	18	12	7
Time-Terms (Seconds)									
BAR	3.77	3.70	3.70	3.57	3.49	3.48	-	-	-
BMT	3.60	3.42	3.42	3.37	3.26	3.25	3.56	3.71	3.75
CAR	3.88	3.78	3.77	3.55	3.61	3.59	3.91	3.95	-
CC	3.78	3.73	3.73	3.83	3.62	3.63	3.57	-	-
CM	3.49	3.33	3.32	3.39	3.14	3.14	-	-	-
DM	3.55	3.53	3.52	3.49	3.24	3.24	3.63	3.66	3.57
GM	3.95	3.94	3.90	3.96	3.72	-	4.03	-	-
LAD	3.69	3.66	3.66	3.57	3.55	-	3.72	3.62	3.67
LPM	3.75	3.66	3.65	3.62	3.56	3.55	3.77	3.81	3.79
SB	4.14	4.02	4.02	3.94	-	-	4.31	4.34	-
SC	3.79	3.79	3.81	3.90	3.74	3.74	3.83	-	-
SMC	4.04	3.93	3.93	3.42	3.38	3.37	-	-	-
TA	3.47	3.36	3.36	3.39	3.12	3.12	-	-	-
WTX	3.63	3.70	3.70	3.70	3.58	3.58	3.65	3.68	3.52
PN1	2.45	2.33	2.30	2.08	1.28	1.22	-	-	-
PN2	2.16	2.06	2.02	1.74	0.64	0.56	-	-	-
PN3	4.44	4.13	4.05	-	-	-	4.85	5.79	3.44
PN4	5.63	-	-	-	-	-	6.18	7.76	3.61
PN5	3.10	2.90	2.85	2.60	1.56	1.49	-	-	-
PN6	5.63	5.19	-	-	-	-	6.09	-	-
PN7	4.43	4.17	4.12	3.76	2.16	-	4.70	5.34	-
PN8	1.81	1.75	1.72	1.44	0.52	0.48	-	-	-
PN9	4.70	4.57	4.56	4.27	3.36	-	-	-	-
PN10	2.89	-	-	-	-	-	3.50	4.83	1.35
PN11	5.57	5.48	5.45	5.31	4.25	-	-	-	-
PN12	0.92	0.79	0.74	0.55	-0.82	-	-	-	-
PN13	1.51	1.37	1.33	1.13	-0.29	-	1.73	-	-
PN14	2.03	1.90	1.85	1.65	0.22	-	2.25	-	-
PN15	1.87	1.74	1.70	1.50	0.09	-	-	-	-
PN16	3.22	-	-	-	-	-	3.93	5.42	1.29
PN17	5.64	-	-	-	-	-	6.30	7.80	3.71
PN18	2.36	-	-	-	-	-	3.08	4.60	4.06
PN19	2.31	2.16	2.12	1.93	0.67	0.60	-	-	-
PN20	3.08	2.90	2.84	2.57	-	-	3.34	4.06	-
PN21	1.41	1.39	1.35	1.42	0.32	0.26	-	-	-
PN22	0.90	0.81	0.78	0.76	-0.27	-0.32	-	-	-
PN23	1.95	1.91	1.87	1.78	0.56	0.50	-	-	-
PN24	0.36	0.23	0.17	-0.13	-	-	6.77	-	-
PN25	6.63	6.38	6.30	-	-	-	6.87	7.78	4.90
PN26	3.53	3.48	3.43	3.24	-	-	-	-	-
PN27	4.17	4.07	4.03	3.96	2.63	2.57	-	-	-

TABLE 21

Readings by Distance for Each Data Set

Distance (km)	Pg upper	Pg lower	P*	PN
	(number of readings)			
0-55	88	0	0	0
(56-75)	15	11	0	0
76-127	0	32	0	0
(128-134)	0	2	11	0
135-192	0	0	54	0
(193-198)	0	0	5	1
199-938	0	0	0	81

( ) overlap between two data sets

TABLE 22

Events Dominated by Readings in a Given Distance Range by Data Set

Distance (km)	Pg upper	Pg lower	P*	Pn
	(number of events)			
0-55	20	0	0	0
(56-75)	1	1	0	0
76-127	0	8	0	0
(128-134)	0	0	2	0
135-192	0	0	23	0
(193-198)	0	0	1	0
199-938	0	0	0	0

( ) overlap between data sites

greater. In the case of all four refractors, adjacent discontinuities have velocities that are seperated by two sigma.

The maximum variation in travel-times for arrivals from different refractors in an overlap zone is 0.15 seconds. This assumes that the crossover distance lies in the middle of the overlap. This difference is less than the uncertainty in timing of arrivals.

A final summary of the results is displayed in Table 23. This lists the time-terms and velocities for the four refractors seen top to bottom, as read from left to right. The first, third and fourth refractors have velocity values that are the most often noted in previous studies, while hints of the second refractor show up in other studies.

TABLE 23

Time-Terms And Velocities For Different Layers

	Pg Upper	Pg Lower	P*	Pn
Velocity (Km/Sec)	5.76±.05	6.25±.08	6.48±.14	8.08±.17
Time-Terms (Seconds)				
BAR	0.40	-	1.73	3.77
BG	0.62	0.67	-	-
BMT	0.10	-	-	3.60
CAR	0.50	-	2.47	3.88
CC	0.28	0.36	1.78	3.78
CM	0.49	0.44	1.86	3.49
CU	0.51	-	-	-
DM	0.44	0.38	-	3.55
FM	0.56	-	-	-
GM	0.26	0.51	2.19	3.95
HC	-	-	2.17	-
IC	0.13	0.55	-	-
LAD	-0.40	0.31	2.33	3.69
LAZ	-	-	3.02	-
LPM	-0.09	0.04	1.84	3.75
NG	0.29	-	1.77	-
RM	0.44	-	1.97	-
SB	0.50	-	3.07	4.14
SC	0.59	0.76	1.78	3.79
SL	0.30	-	-	-
SMC	0.44	-	3.11	4.04
SNM	-	0.37	-	-
TA	-	-	-	3.47
WM	0.19	-	-	-
WTX	0.08	0.49	2.15	3.63

INTERPRETATION OF RESULTS

Introduction

The major question concerning the results of this study is whether they compare favorably with previous results, and how do structural models derived from the time-terms and velocities compare with known geologic and crustal structure? The time-terms can be thought of as delay times. Using notation from Berry and West (1966), the formula for the thickness of layer one is

$$d_1 = a_1 \frac{V_1 V_2}{[V_2^2 - V_1^2]^{\frac{1}{2}}} = a_1 K[V_2, V_1] \qquad (17)$$

where $K[V_2, V_1] = \frac{V_1 V_2}{[V_2^2 - V_1^2]^{\frac{1}{2}}}$.

$K[V_2, V_1]$ is the time-term conversion factor. The equation for the thickness for the second layer is

$$d_2 = \{a_2 - [d_1 / K(V_3, V_1)]\} K[V_3, V_2] . \qquad (18)$$

The general formula for depth to a given layer is

$$H = \sum_{j=1}^{N} d_j = \sum_{j=1}^{N} \left\{ a_j - \sum_{i=1}^{j-1} d_i / K[V_{j+1}, V_i] \right\} K[V_{j+1}, V_j] \qquad (19)$$

(Berry and West, 1966). The above formula requires that the top layers are calculated first and the successively lower

layers next.

Before presenting the interpretation, depth uncertainties must be mentioned. Two factors influence the uncertainty of a time-term; local effects (reading error, near-surface geological complexities) and uncertainty in velocity. Smith et al. (1966) present the following equation that relates time-term and velocity uncertainties

$$\delta b_v = \frac{\bar{\Delta}}{V} \delta V, \qquad (20)$$

where δb_v is the time-term uncertainty, $\bar{\Delta}$ is the average distance between a station and sources, V is the refractor velocity and δV is the uncertainty in velocity. A conservative formulation is to sum the uncertainties when calculating depth uncertainty

$$\delta \text{Depth} = \{ (\delta b_L + \delta b_v)/b \} \text{depth}. \qquad (21)$$

δb_L is uncertainty in time-term due to local effects. This is the uncertainty calculated by the computer program during the general inversion of the data. b is the time-term. These are one sigma uncertainties for the depth calculation, as is the case for the time-term and velocity uncertainties.

Precambrian Surface

Figure 10, from Chapin et al. (1978), suggests that a number of cauldrons occur southwest and west of Socorro. Stations SB,WM,NG,CM,SC,IC and RM lie in, or on an edge of one of these cauldrons. The thickness of 3.4 km/sec material below these stations ranges from 547 to 2484 meters (Table 24). The results of this study indicate that stations IC, NG, and WM probably lie over the resurgent dome for the Socorro cauldron because these sites have a significantly thinner layer of post-collapse material (550-1200 meters) than stations RM, SC and CM (1850-2500 meters) (see Table 24 for individual values of thickness). Because of large surface elevation variations in the area, plots of the elevation for each refractor are made rather then the depth of each refractor. All elevations given in Tables 28 to 30 and Figures 11,13,14 and 15 are relative to sea level. As can be seen in Figure 11 and Table 26, the elevation of the bottom of the fill is 1.2 km at IC, 0.9 km at WM and 0.5 km at NG. These stations lie over the resurgent dome and towards the middle of the Socorro cauldron. The bottom of the fill for stations near the edges of the Socorro cauldron is -0.1 km at RM and -0.4 km at both SC and CM. The depths show that the resurgent dome has relief relative to the lowest points of the moat of at least 1.6 km.

Figure 2. Overlapping and nested cauldrons and a transverse shear zone (double line) in the Socorro-Magdalena area. Base is composite of Socorro and Tularosa 2-degree quadrangles (Army Map Service plastic relief maps). From oldest to youngest, the cauldrons and their ash-flow tuff sheets are: 1) Nogal Canyon—Vicks Peak, 2) North Baldy—Hells Mesa, 3) Mt. Withington—A-L Peak Tuff, granophyre member, 4) Magdalena—A-L Peak Tuff, flow-banded member, 5) Sawmill Canyon—A-L Peak Tuff, pumiceous member, 6) Mt. Withington—Pozo Canyon Tuff, 7) Socorro— tuff of Lemitar Mountains, 8) Hop Canyon—tuff of South Canyon. Nogal Canyon and Mt. Withington cauldrons after Deal and Rhodes (1976).

Figure 10. Cauldrons that lie in the Socorro, New Mexico area (from Chapin et al., 1978).

TABLE 24

Thickness Of Rock Which Has Velocity Of 3.4 km/sec from Time-Terms and Upper Crustal Velocity

Station ID	Depth To Basement If Velocity Is 5.76 km/sec
BAR	1684±589 meters
BG	2610±505 meters
BMT	421±674 meters
CAR	2105±505 meters
CC	1179±421 meters
CM	2063±463 meters
CU	2147±547 meters
DM	1852±421 meters
FM	2358±421 meters
GM	1095±716 meters
IC	547±463 meters
LAD	0±800 meters
LPM	0±716 meters
NG	1221±589 meters
RM	1852±589 meters
SB	2105±463 meters
SC	2484±463 meters
SL	1263±463 meters
SMC	1852±379 meters
WM	800±589 meters
WTX	337±294 meters

TABLE 25

Depth To The 6.25 km/sec Discontinuity Using Time-Terms and Three-Layer Model Layer One Velocity Is 3.4 Km/Sec, Layer Two Velocity Is 5.76 Km/Sec, and Layer Three Velocity Is 6.25 Km/Sec

Station ID	Layer One Thickness (meters)	Layer Two Thickness (meters)	Depth To 6.25 km/sec (meters)
BG	2610	4437	7047±2967
CC	1179	5029	6208±3395
CM	2063	2810	4873±2707
DM	1852	2662	4757±1879
GM	1095	7543	8638±3936
IC	547	10353	10900±4727
LAD	0	8726	8726±4585
LPM	0	4733	4733±4289
SC	2484	6064	8548±2876
WTX	337	10205	10542±4244

Note about 2/3 of the uncertainty of depth is due to the uncertainty of velocity.

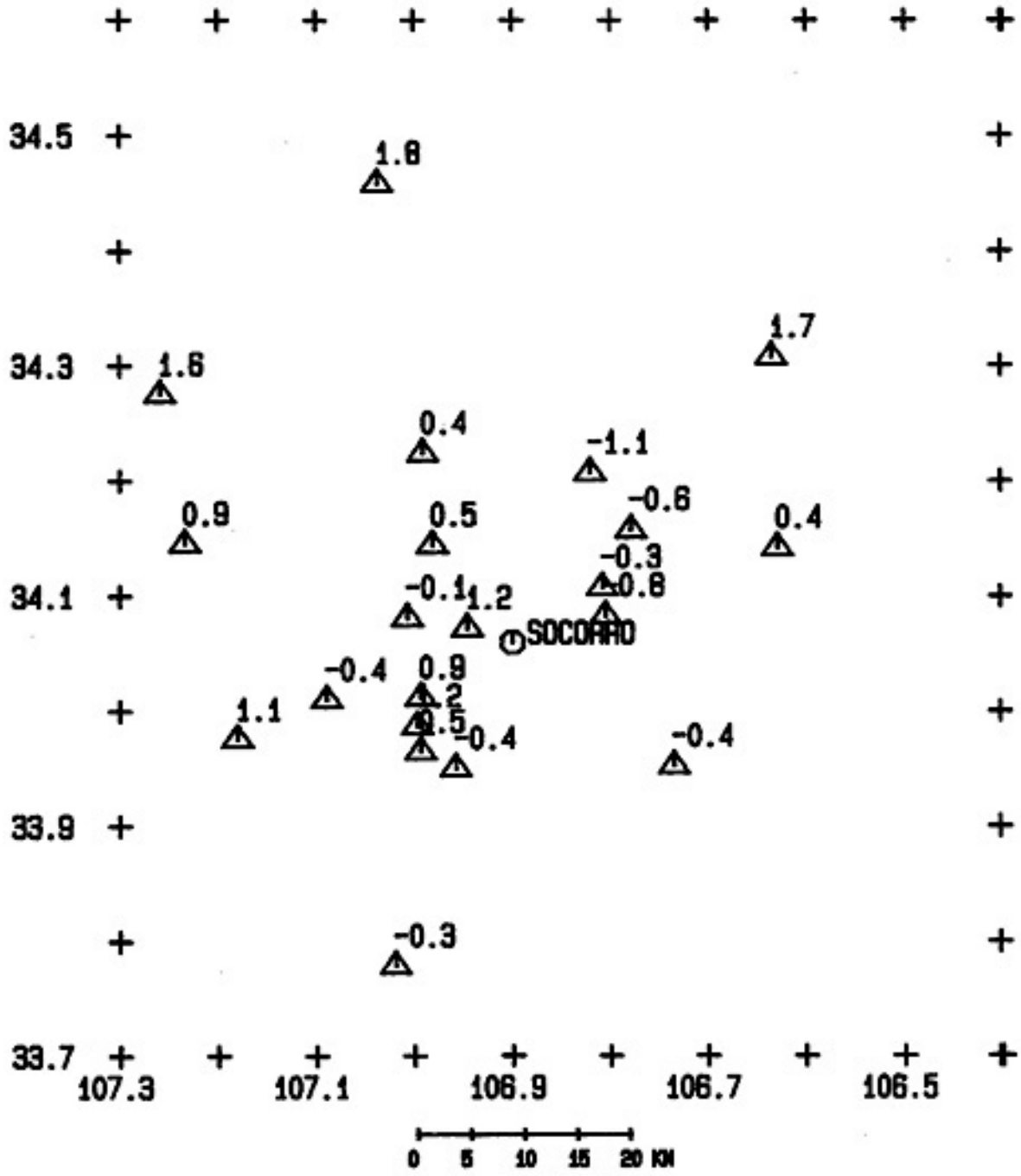

Figure 11. Elevation of the 5.76 km/sec refractor, based on depths in Table 24. All numbers are elevation in km relative to sea level.

TABLE 26

Model Elevations Relative To Sea Level
Elevation Of The Top Of The Paleozoic/Precambrain Surface

Station ID	3.4 Km/Sec Over 5.76 Km/Sec (km)
BAR	+0.4
BG	-1.1
BMT	+1.6
CAR	-0.4
CC	+0.5
CM	-0.4
CU	-0.6
DM	-0.3
FM	-0.8
GM	+0.9
IC	+1.2
LAD	+1.8
LPM	+1.7
NG	+0.5
RM	-0.1
SB	+1.1
SC	-0.4
SL	+0.4
SMC	-0.3
WM	+0.9
WTX	+1.2

Another area on Figure 11 shows that the elevation of the basement is consistently below sea level along a line of stations. BG, FM, DM and CU have basement elevations of -0.3 to -1.1 km . This means that the Precambrian rock lies 1.8 to 2.6 km below these stations.

Areas outside of those mentioned above have basement elevations 0.5 km or above. Both LAD and LPM, according to the calculations, must rest on basement outcrops; this agrees with the known geology.

The velocity of 5.76±0.05 km/sec determined by the time-term method for events nearer than 75 km is in agreement with values found in previous studies (Table 2). It is only slightly lower than the value obtained by Ward (1980) of 5.85±0.02 km/sec which resulted from the most comprehensive study to date. The time-terms and station corrections (Ward, 1980) have the same pattern (see Figures 2 and 3). Both have large values and small values in the same areas. Larger positive correction factors exist for stations on the edge of the Socorro cauldron (SC, CM and RM) than for stations in the middle (NG, IC and WM) which indicates greater fill thickness on the edges of the cauldron than in the middle.

A final question is whether any of the dips in the basement refractor exceed the 10 degree limit which can cause significant errors according to Reiter (1970). Between SC and IC there is a difference in elevation of the

Precambrian of 1.6 km over a distance of 3.9 km, which results in a dip of 24 degrees. If you use the pair WTX and SC an elevation difference of 1.6 km exists, and the distance difference is 8.1 km which yields a dip of 11 degrees. When looking over the whole set of possible station pairs for the two sources, there are only 36 out of 186 combinations which have dips over 10 degrees. In fact, for the San Marcial shots, none of the station pairs yield dips over six degrees. For the stations where dips exceed 10 degrees, the depths calculated by the time-term method will be too small (Reiter, 1970).

The 6.25 km/sec Discontinuity

Using explosions at 56-135 km from the stations, the velocity of the Pg phase is 6.25±0.08 km/sec. This is over one standard deviation higher than any value for Pg velocity in the Rio Grande rift listed in Table 2. In past studies, measured Pg velocities occurred in two groups, one averaging 5.8 km/sec and the other 6.1 km/sec. This may indicate there are really two layers in the upper crust between the Conrad and Phanerozoic rocks. To determine if the time-terms listed in Table 7 are relative or nearly absolute, the average depth is calculated. Depth to the 6.25 km/sec discontinuity is 3.4±2.8 km when using equation (19).

Using the above depth to the 6.25 km/sec discontinuity and 1.2 km for the average depth to the Precambrian discontinuity, the resulting crossover distance on a travel-time versus distance graph is about 15 km, which is far too small. If the crossover distance is 15 km, the time-term at LPM should be more negative than it is. This also does not fit with Ward (1980) who found a Pg velocity of 5.85 km/sec for earthquakes which were commonly at distances greater than 15 km from stations. To find the true crossover distance, a plot of travel-time versus distance was made using both sets of Pg data (Figure 12). The crossover point lies somewhere between 54 and 62 km (depth calculations use 58 km as the crossover distance). Below is the equation for the thickness of the first layer (3.4 km/sec material) (Dobrin, 1976).

$$Z_1 = \frac{1}{2}\sqrt{\frac{V_2-V_1}{V_2+V_1}}\, X_{cross} \quad . \qquad (22)$$

The above equation yields an average Phanerozoic thickness of 2.01 km for sources and stations which can be compared to 1.01 km obtained for the stations by the time-term method. For the second layer (5.76 km/sec) the following equation derived from standard equations (Dobrin, 1976) was used:

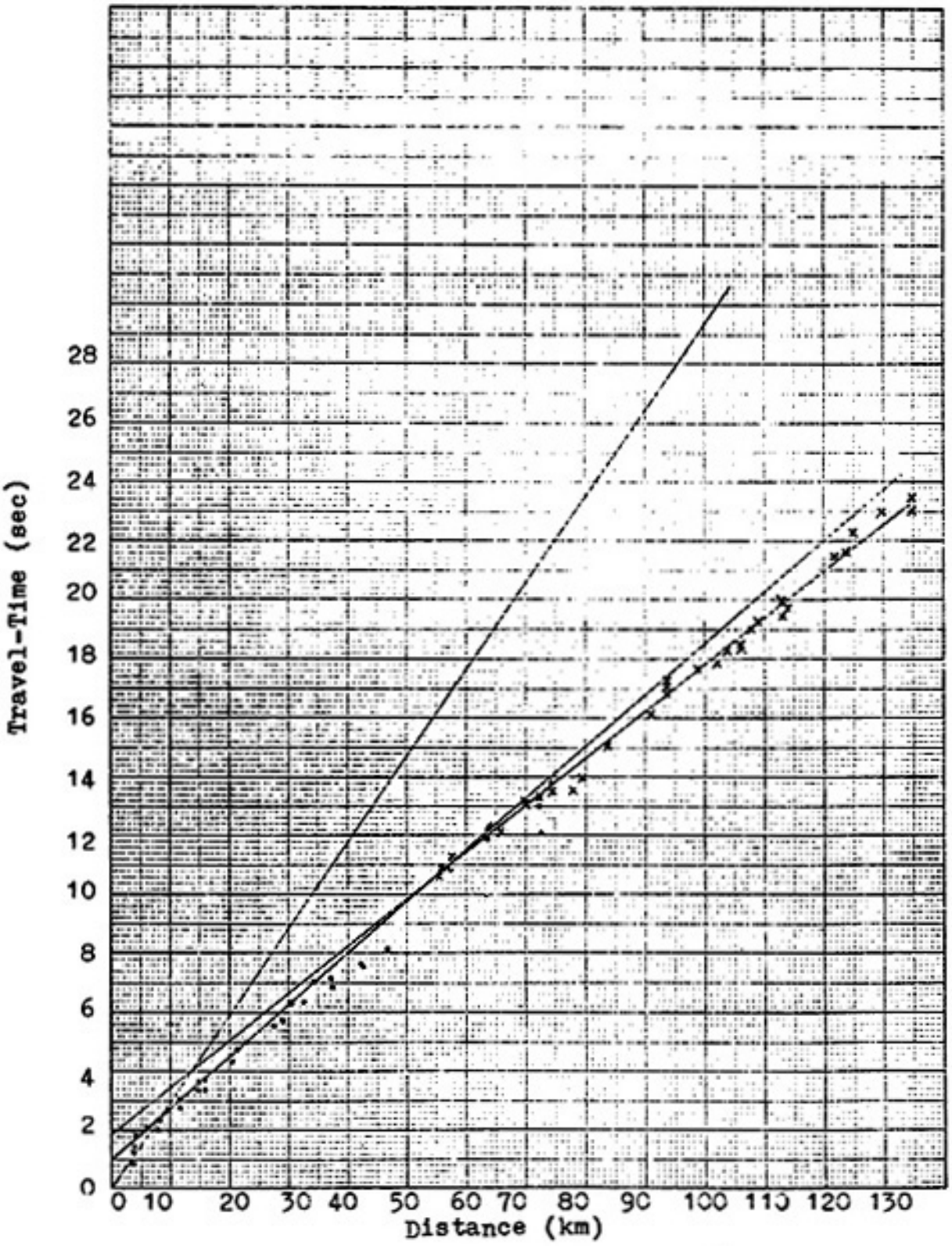

Figure 12. Travel-time vs. epicentral distance for Pg arrivals. Dots are for TERA and San Marical shot, while x's are for Jackpile Mine, White Sands Missile Range or Kirtland Air Force Base shots.

$$\left\{ \frac{X_{cross\,2}}{V_2} - \frac{X_{cross\,1}}{V_1} + \frac{2Z_1\sqrt{V_2^2-V_1^2}}{V_2 V_1} - \frac{2Z_1\sqrt{V_3^2-V_1^2}}{V_3 V_1} \right\} \frac{V_3 V_2}{\sqrt{V_3^2-V_2^2}} = Z_2 \quad (23)$$

The above equation gives a depth effected by both source and stations. Using the above equation, Z is 6.04 km and the total depth to the 6.25 km/sec discontinuity is 8.05 km. If the lowest value for the crossover distance is used, the depth to the 6.25 km/sec discontinuity is 7.49 km, and for the largest crossover distance, it is 8.48 km. A depth of 8.05 km gives a time-term of 0.73 seconds. This is 0.28 seconds larger than the one derived by the time-term method. To find depth at any given station to the 6.25 km/sec discontinuity, the difference of the two values was added to each time-term from Table 7 to yield the results listed in Table 25. The elevation the 6.25 km/sec discontinuity is lowest under WTX and IC. In general this surface is dipping toward the west (see Figure 13).

The two refractor velocities for the upper crust indicate that there is a composition change. The 5.76 km/sec refractor velocity is near the average of granite velocities shown in Table 18 of Carmichael (1982) which is 5.62 km/sec. An average diorite velocity in Table 18 of Carmichael (1982) is 6.27 km/sec which is close to the velocity of the second layer in the upper crust, 6.25 km/sec.

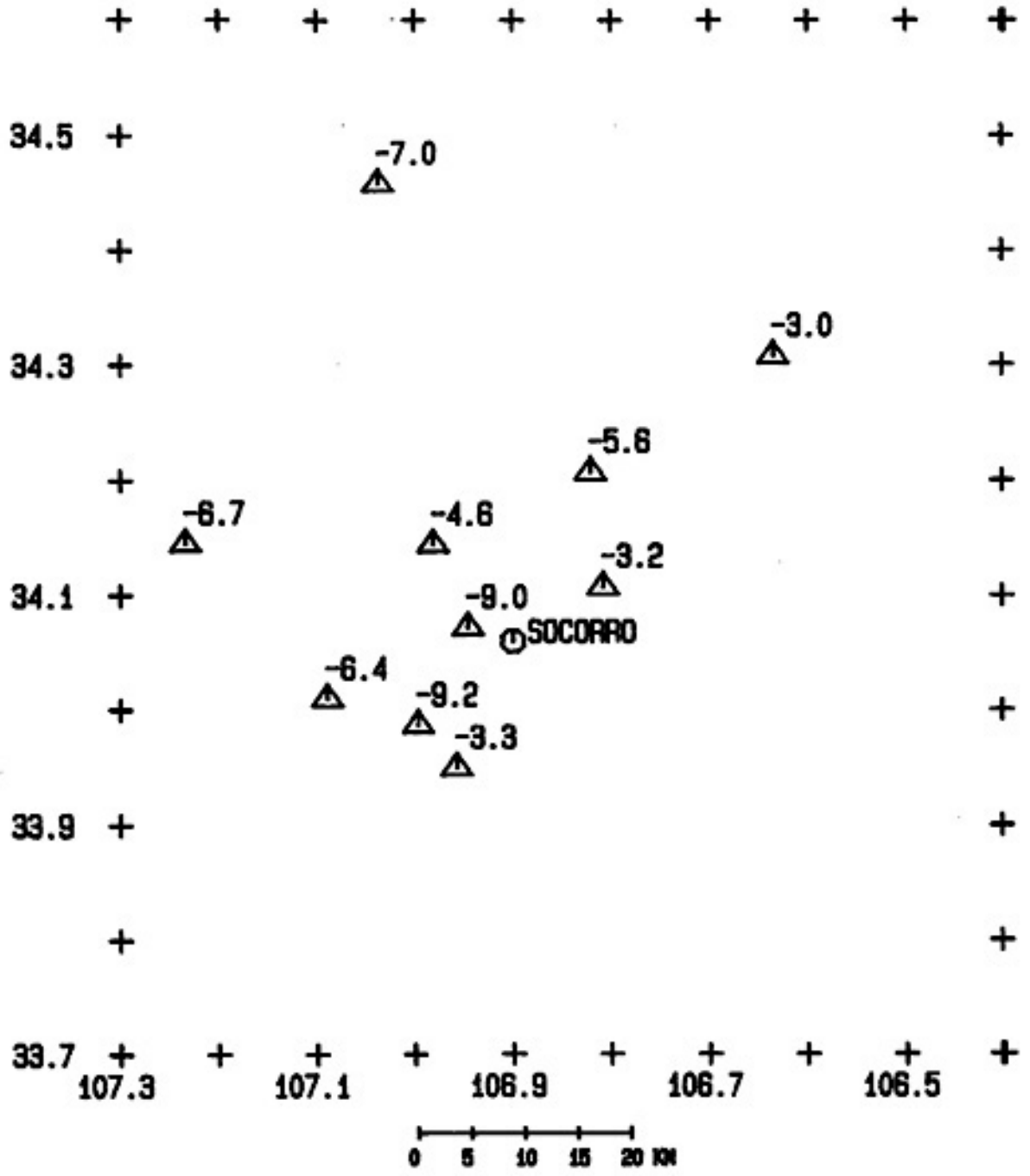

Figure 13. Elevation of the 6.25 km/sec refractor, using depths in Table 25. All numbers are elevation in km relative to sea level.

The Conrad Discontinuity

Because there are no sites which have both a source and a receiver, all time-terms calculated are arbitrary and relative to a tie between LPM and WTX which uses 6.5 km/sec as the refractor velocity and a time-term of two seconds for both WTX and LPM. Velocity is independent of time terms if they are relative or absolute. The velocity for this refractor is 6.48 ± 0.17 km/sec and the relative time-terms range from 1.7 to 3.1 seconds. The velocity found along the Conrad discontinuity is very similar to that in other studies (Table 2). The relative time-terms can provide some information on the relief of the Conrad discontinuity, but no information about its absolute depth. As can be seen in Figure 7, there seems to be little pattern in the relative time-terms. Toppozada and Sanford (1976) obtained a value for upper crustal thickness of 18.6 km which will be used below in the calculations for the depth of the Moho.

The Moho Discontinuity

The final discontinuity studied was the Moho. Tables 27 and 28 are Moho depths calculated when using four and five layer models, respectively. The velocity of 8.08 km/sec agrees with eight previous studies which measured Pn

TABLE 27

Depth To The Moho Using A Four Layer Model
Layer One Velocity Is 3.4 Km/Sec, Layer Two Velocity Is 5.76 Km/Sec
Layer Three Velocity Is 6.48, Layer Four Velocity Is 8.08 Km/Sec

Station ID	Thickness Of Layer One (km)	Thickness Of Layer Two* (km)	Thickness Of Layer Three (km)	Depth To Moho (km)
BAR	1.7	16.9	13.9	32.5±8.7
BMT	0.4	18.2	14.2	32.8±14.3
CAR	2.1	16.5	14.4	33.0±9.7
CC	1.2	17.4	14.9	33.5±8.8
CM	2.1	16.5	10.2	28.8±12.5
DM	1.9	16.7	11.3	29.9±12.1
GM	1.1	17.5	16.8	35.4±12.1
LAD	0.0	18.6	15.8	34.4±11.0
LPM	0.0	18.6	16.5	35.1±12.8
SB	2.1	16.5	17.4	36.0±14.4
SC	2.5	16.1	12.8	31.4±10.4
SMC	1.9	16.7	16.6	35.2±9.9
WTX	0.3	18.3	14.6	33.2±14.5

*note used Toppozada and Sandford (1976) value for depth to the Conrad, which is 18.6 km. At least 4/5 of the depth uncertainty is due to velocity uncertainty.

TABLE 28

Depth To The Moho Using A Five Layer Model
Layer One Velocity Is 3.4 Km/Sec, Layer Two Velocity Is 5.76 Km/Sec
Layer Three Velocity Is 6.25 Km/Sec, Layer Four Velocity 6.48 Km/Sec
And Layer Five Velocity Is 8.08 Km/Sec

Station ID	Layer One Thickness (km)	Layer Two Thickness (km)	Layer Three Thickness (km)	Layer Four Thickness (km)	Depth To Moho (km)
CC	1.2	5.0	12.4	17.6	36.2±9.5
CM	2.1	2.8	13.7	13.1	31.7±13.7
DM	1.9	2.7	14.0	14.3	32.9±13.3
GM	1.1	7.5	10.0	19.0	37.6±13.1
LAD	0.0	8.7	9.9	18.0	36.6±11.7
LPM	0.0	4.7	13.9	19.5	38.1±13.9
SC	2.5	6.1	10.0	15.0	35.6±11.7
WTX	0.3	10.2	8.1	16.5	35.1±15.4

*see note of table 26 about Conrad and depth uncertainties

velocities (Table 3). All eight of the latter values are within the uncertainty, one sigma, of a velocity of 8.08 km/sec obtained in this study, while the other three (5, 6 and 9) differ by more than two sigma from this velocity.

Assuming Phanerozoic rock with a velocity of 3.4 km/sec, a two-layered crust with an upper-crust velocity of 5.76 km/sec, a lower-crust velocity of 6.48 km/sec, and a Pn velocity of 8.08 km/sec, the calculated crustal thicknesses range from 29-36 km, with an average of 33.2 km (Table 27). The average crustal thickness from previous studies in the Rio Grande rift is 34 km (Table 3).

The last model included five layers (Table 28). In this model, some of the upper crust has a velocity of 6.25 km/s rather than 5.76 km/sec. The calculated thicknesses are significantly increased and range from 31.7 to 38.1 km. with an average of 35.5 km. This is similar to 30-36 km range of crustal thickness along Line 2A of the COCORP study (Brown et al., 1979).

Maps are presented of the Moho elevation relative to sea level to avoid any distortion of mantle relief due to about 1.5 km of surface relief. Figures 14, and 15 show the elevation of the Moho (8.08 km/sec refractor) for the two different models. Elevations are also listed in Table 30 for convenient comparison among the two models. For the four-layer model (Figure 14) the Moho has its highest elevations in the middle of the study area and dips off in

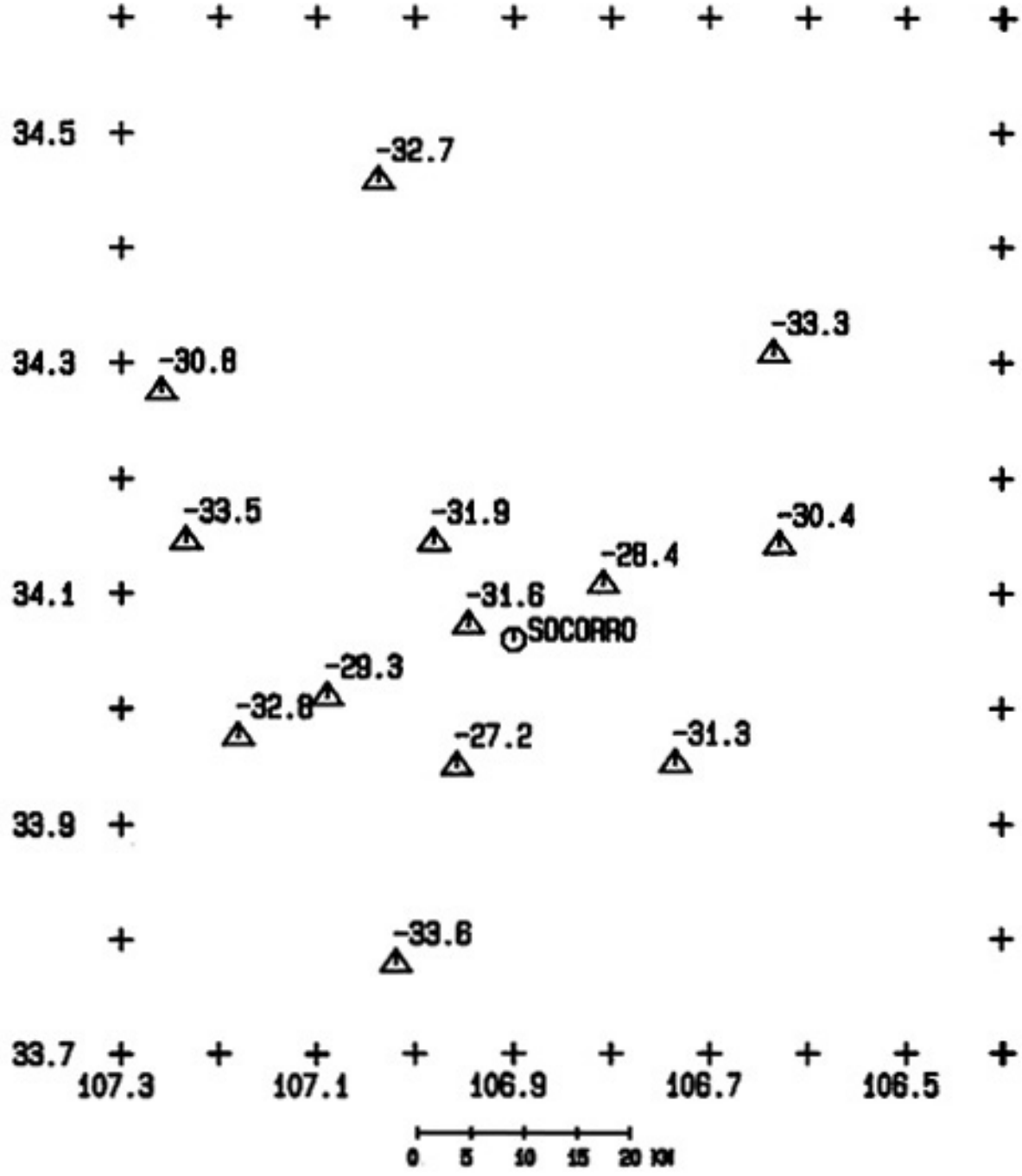

Figure 14. Elevation of the Moho using the four-layer model of Table 26. All values are elevation in km relative to sea level.

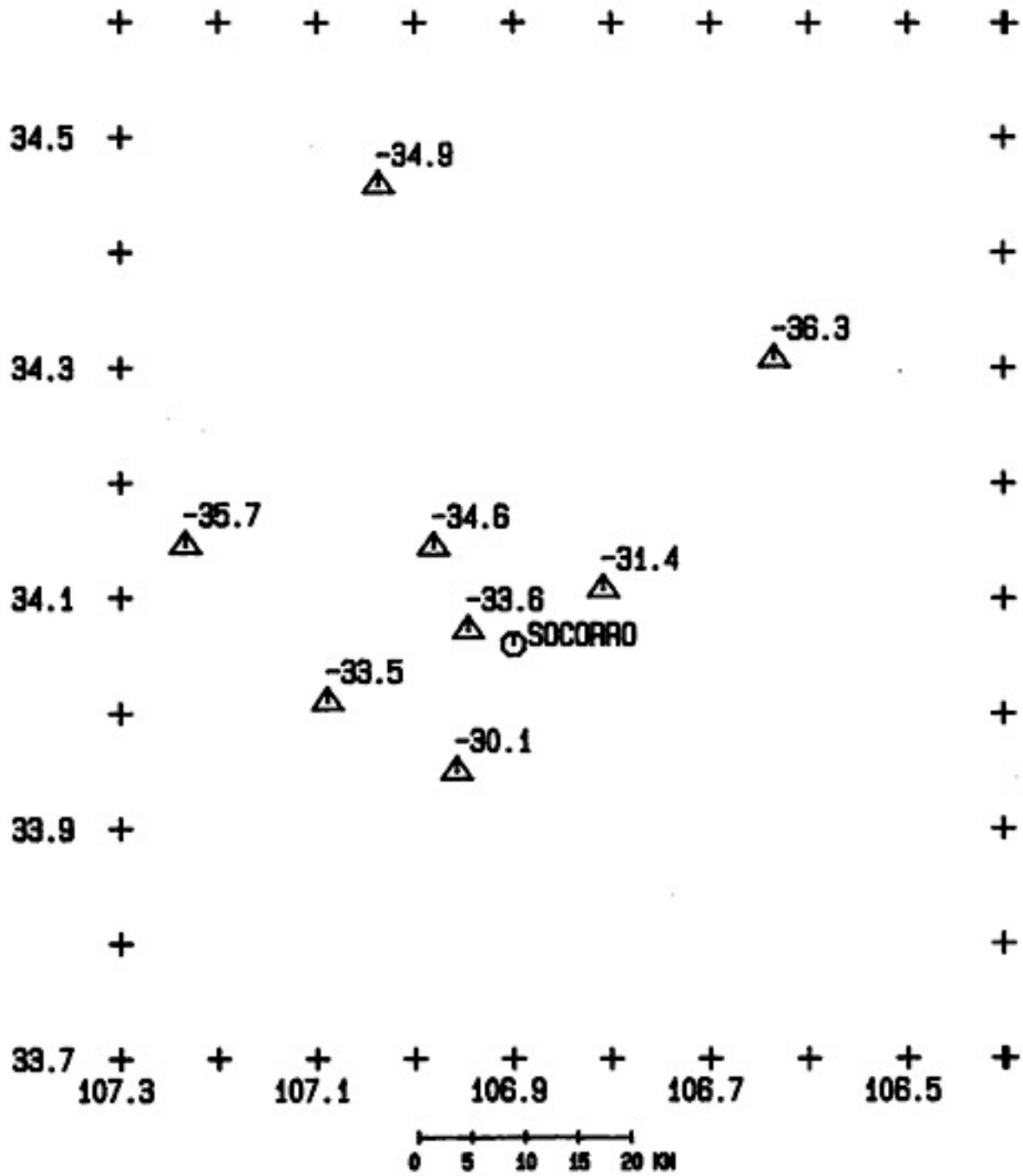

Figure 15. Elevation of Moho, using the five-layer model of Table 27. All values are elevation in km relative to sea level.

TABLE 29

Elevation To The Top The 6.25 km/sec
Discontinuity Relative To Sea Level
Using Model Noted In Table 23

Station ID	Elevation Of 6.25 km/sec Discontinuity (km)
BG	-5.6
CC	-4.6
CM	-3.3
DM	-3.2
GM	-6.7
IC	-9.2
LAD	-7.0
LPM	-3.0
SC	-6.4
WTX	-9.0

TABLE 30

Elevation To The Top The Mantle
Relative To Sea Level
Using Models Of Table 24,25 AND 26

Station ID	Model 24 (km)	Model 25 (km)
BAR	-30.4	--
BMT	-30.8	--
CAR	-31.3	--
CC	-31.9	-34.6
CM	-27.2	-30.1
DM	-28.4	-31.4
GM	-33.5	-35.7
LAD	-32.7	-34.9
LPM	-33.3	-36.3
SB	-32.8	--
SC	-29.3	-33.5
SMC	-33.6	--
WTX	-31.6	-33.6

all directions. This peak lies beneath stations DM,CM and SC. For the five-layer model (Figure 15) the Moho dips to the north-northwest. This dip to the north for the Moho was also reported by Toppozada and Sanford (1976).

SUMMARY

Pn, P* and Pg waves, which are head-waves that travel along the Moho, Conrad and basement respectively, were studied using the time-term method. (The computer program used in this study is listed in Appendix B.) The resulting velocities for Pg arrivals were: (1) 5.76±0.05 km/sec for shots within 75 km of stations and (2) 6.25±0.08 km/sec for explosions between 56 and 135 km from stations. The 5.76 km/sec velocity is similar to values obtained in previous studies. The 6.25 km/sec material is in the lower part of the upper crust.

The thickness of the low-velocity Phanerozoic material agrees well with the observed geology and with results from previous studies. Mesozoic-Paleozoic material near the Rio Grande rift is at least 1-2.5 km thick. Deposits in the Socorro cauldron are 0.5-2.5 km thick. They are thickest near the edge of the cauldron and thinnest over a hypothesized resurgent dome near the center of the cauldron.

The velocity at the Conrad discontinuity is 6.48±0.14 km/sec which again agrees with previous studies. Since the study of travel-times for the P* arrival only produced relative time-terms, nothing can be said about depth to the Conrad.

The velocity beneath the Moho was found to be 8.08±0.17 km/sec. If the model for the crust includes Phanerozoic rock (3.4 km/sec), an upper crust with a velocity of 5.76 km/sec, a lower crust with a velocity of 6.48 km/sec and a upper mantle with a velocity of 8.08 km/sec, the crustal thickness ranges from 28.8-36.0 km with an average of 33.2 km. These are close to most of the crustal thicknesses obtained in previous studies. Results may delineate a pattern of thinner crust under the Rio Grande rift and Socorro cauldron.

In conclusion, the time term method, when used to study refraction data, can yield results which are generally consistant with those obtained by other geophysical and geological methods. In order to get more detailed information on the geologic and crustal structure in the Socorro area, more data is necessary both in number of events recorded at each station and in the number of different stations recording the events.

REFERENCES

Barr, K.G.,(1971), The statistics of the time-term method, Bulletin of the Seismological Society of America. 61, 1853-1854.

Berry, M.J. and G.F. West, (1966), An interpretation of the first-arrival data of the Lake Superior experiment by the time-term method, Bulletin of the Seismological Society of America. 56, 141-171.

Brown, L.D. P.A. Krumhansl, C.E. Chapin, A. Sanford, F.A. Cook, S. Kaufman, J.E. Oliver and F.S. Schilt, (1979), COCORP seismic reflection studies of the Rio Grande rift, in Riecker, R.E. ed., Rio Grande Rift: Tectonics and Magmatism,American Geophysical Union Special Publication, 169-184.

Brown, L.D., C.E. Chapin, A.R. Sanford, S. Kaufman and J. Oliver, (1980), Deep structure of the Rio Grande Rift from seismic reflection profiling, Journal of Geophsyical Research. 85, 4773-4800.

Cape, Cheryl, Susan McGeary and George Thompson, (1983), Cenozoic normal faulting and the shallow structure of the Rio Grande rift near Socorro, New Mexico, Geological Society Of America Bulletin. 94, 3-14.

Carmichael, Robert S. ed., (1982), Handbook of Physical Properties of Rocks Volume II, CRC Press, Inc.

Chapin, C.E., (1979), Evolution of the Rio Grande rift, in Riecker, R.E. ed., Rio Grande Rift: Tectonics and Magmatism, American Geophysical Union Special Publication, 1-5.

Chapin, C.E., R.M. Chamberlain, G.R. Osburn, D.W. White and A.R. Sanford, (1978), Exploration framework of the Socorro geothermal area, New Mexico, New Mexico Geological Society Special Publication. 7,114-129.

Cook, Frederick A., Dan B. McCullar, Edward R. Decker, and Scott B. Smithson, (1979), Crustal structure and evolution of the southern Rio Grande rift, in Riecker, R.E. ed., Rio Grande Rift: Tectonics and Magmatism, American Geophysical Union Special Publication, 195-204.

Dobrin, Milton B., (1976), Introduction to Geophysical Prospecting, Mc Graw Hill Book Company.

Draper, N. and H. Smith, (1966), Applied Regression Analysis, John Wiley and Sons.

Gish, D.M., G.R. Keller and M.L. Sbar, (1981), A refraction study of deep crustal structure in the Basin and Range: Colorado Plateau of eastern Arizona, Journal of Geophysical Research. 86, 6029-6038.

Jaksha, L.H., (1982), Reconnaissance seismic refraction-reflection surveys in southwestern New Mexico, Geological Society of America Bulletin. 93, 1030-1037.

Keller, G.R., L.W. Brailes and J.W. Schlue, (1979), Crustal structure along the Rio Grande rift from surface wave dispersion measurements, in Riecker, R.E. ed., Rio Grande Rift: Tectonics and Magmatism, American Geophysical Union Special Publication 115-126.

McCollom, Robert L., and Robert S. Crosson, (1975), An array study of upper mantle velocity in Washington state, Bulletin of the Seismological Society of America. 65, 467-482.

McCullar, D.B. and S.B. Smithson, (1977), Unreversed seismic crustal refraction profile across the southern Rio Grande rift (abstract) EOS. 58, 1184.

Murdock, J.N. and L.H. Jaksha, (1978), Estimates of relative time terms and of Pn velocity in central New Mexico (abstract), Proc. Rio Grande Rift Symp., 63.

Murdock, J.M. and L.H. Jaksha, (1980), Time term solutions and corresponding data for the crustal structure of north central New Mexico, U.S. Geological Survey Open-File Report 80-2014.

Olsen, K.H., G.R. Keller, and J.N. Stewart, (1979), Crustal structure along the Rio Grande rift from seismic refraction profiles, in Riecker, R.E. ed., Rio Grande Rift: Tectonics and Magmatism, American Geophysical Union Special Publication, 127-144.

Phinney, R.A., (1964), Structure of the earth's crust from spectral behaviour of long-period body waves, Journal of Geophysical Research. 69, 2997-3017.

Reagor, B.G., D.W. Gordon, and J.N. Jordan, (1968), Seismic analysis of a nuclear explosion: Gasbuggy, USCGS Seismology Division, Washington, D.C., 73 pp.

Reiter, Leon, (1970), An investigation into the time term method of refraction seismology, Bulletin of the Seismological Society of America. 62, 1-13.

Rinehart, Eric J., Allan R. Sanford, and Roger Ward, (1979), Geographic and extent shape of an extensive magma body at mid-crustal depths in the Rio Grande rift near Socorro, New Mexico, in Riecker, R.E. ed., Rio Grande Rift: Tectonics and Magmatism, American Geophysical Union Special Publication, 237-252.

Sanford, Allan R., (1978), Characteristics of Rio Grande rift in vicinity of Socorro, New Mexico, From Geophysical Studies, New Mexico Bureau of Mines Circular 163, 116-121.

Sanford, A.R., R.P. Mott, Jr., P.J. Shuleski, E.J. Rinehart, F.J. Caravella, R.M. Ward, and T.C. Wallace, (1977), Geophysical evidence for a magma body in the crust in the vicinity of Socorro, New Mexico, American Geophysical Union, Geophysical Monograph 20, 385-403.

Smith, Jefferson T., John Steinhart, and L.T. Aldrick, (1966), Lake Superior Crustal Structure, Journal of Geophysical Research, 71, 1141-1173.

Stewart, S.W. and L.C. Pakiser, (1962), Crustal structure in eastern New Mexico interpretated from the Gnome explosion, Bulletin of the Seismological Society of America. 52, 1017-1030.

Tatel, H.E., and M.A. Tuve, (1955), Seismic exploration of a continental crust, Geological Society Of America Special Paper. 62, 35-50.

Toppozada, T.R., (1974), Seismic investigation of crustal structure and upper mantle velocity in the state of New Mexico and vicinity, Ph.D. Dissertation, New Mexico Institute of Mining and Technology, 152 pp.

Toppozada, Tousson R. and Allan R. Sanford, (1976), Crustal structure in central New Mexico interpreted from the Gasbuggy explosion, Bulletin of the Seismological Society of America. 66, 877-886.

Ward, R.M., (1980), Determination of three-dimensional velocity anomalies within the upper crust in the vicinity of Socorro, New Mexico using first P-arrival times from local earthquakes, Ph.D. Dissertation, New Mexico Institute of Mining and Technology.

Ward, R.M., J.W. Schlue and A.R. Sanford, (1981), Three-dimensional velocity anomalies in the upper crust near Socorro, New Mexico, Geophysical Research Letters. 8, 553-556.

Warren, D.H. and W.H. Jackson, (1968), Surface seismic measurements of the project Gasbuggy explosion at intermediate distance ranges, U.S. Geological Survey Open File Report, 45 pp.

Willmore, P.L. and A.M. Bancroft, (1960), The time term approach to refraction Seismology, Geophysics Journal. 3, 419-432.

Appendix A

a) Table A is a list of readings used for Pg arrivals for events less than 75 km from the stations.

b) Table B is a list of readings used for Pg arrivals for events which are between 56 and 135 km from the stations.

c) Table C is a list of readings used for the P* study.

d) Table D is a list of readings used for the Pn study.

TABLE A

Pg Readings From Near By Shots

Event	Station	Arrival-Time (hour:mon:sec)	Travel-Time (seconds)	Distance Traveled (km)
PGS1	CC	16:51:53.66	2.62	11.8
PGS1	SC	16:51:53.91	2.87	12.1
PGS1	FM	16:51:54.45	3.41	15.4
PGS2	WTX	18:56:13.68	1.24	4.0
PGS2	CC	18:56:15.19	2.75	11.8
PGS2	DM	18:56:16.18	3.74	16.2
PGS2	SL	18:56:16.87	4.43	20.6
PGS2	BG	18:56:17.48	5.04	22.8
PGS2	CU	18:56:17.11	4.67	21.5
PGS3	WTX	19:16:44.83	1.24	4.0
PGS3	CC	19:16:46.29	2.70	11.8
PGS3	DM	19:16:47.32	3.73	16.2
PGS3	SL	19:16:47.86	4.27	20.6
PGS3	BG	19:16:48.61	5.02	22.8
PGS3	CU	19:16:48.31	4.72	21.5
PGS4	WTX	19:45:28.69	1.24	4.0
PGS4	DM	19:45:31.12	3.67	16.2
PGS4	CC	19:45:30.28	2.83	11.8
PGS4	SL	19:45:31.73	4.28	20.6
PGS5	WTX	18:47:55.12	1.24	4.0
PGS5	IC	18:47:55.89	2.01	8.2
PGS5	CM	18:47:56.50	2.62	9.9
PGS5	CC	18:47:56.67	2.79	11.8
PGS5	SC	18:47:57.00	3.12	12.1
PGS6	IC	18:49:00.40	1.92	8.2
PGS6	CM	18:49:01.10	2.62	9.9
PGS	CC	18:49:01.10	2.62	11.8
PGS6	SC	18:49:01.60	3.12	12.1
PGS7	WTX	23:48:25.93	1.24	4.0
PGS7	WM	23:48:26.09	1.40	4.1
PGS7	RM	23:48:26.70	2.01	6.2
PGS7	NG	23:48:26.99	2.30	8.7
PGS7	FM	23:48:28.46	3.77	15.4
PGS8	WTX	20:43:27.16	1.24	4.0
PGS8	FM	20:43:29.62	3.70	15.4
PGS8	GM	20:43:31.45	5.53	27.7
PGS9	WTX	19:50:29.42	0.86	3.7
PGS9	FM	19:50:31.86	3.30	15.9
PGS10	WTX	22:49:52.34	0.86	3.7
PGS10	DM	22:49:54.80	3.32	15.9
PGS10	FM	22:49:54.79	3.31	15.1
PGS11	CC	19:48:00.14	2.69	11.8
PGS11	BG	19:48:02.36	4.91	22.8
PGS11	SL	19:48:01.70	4.25	20.6
PGS11	LAD	19:48:05.55	8.10	47.0
PGS11	LPM	19:48:05.05	7.60	42.5
PGS12	CC	23:23:26.23	2.69	11.8
PGS12	BG	23:23:28.48	4.94	22.8
PGS12	SL	23:23:27.75	4.21	20.6
PGS12	LAD	23:23:31.65	8.11	47.0

Event	Station	Arrival-Time (hour:min:sec)	Travel-Time (seconds)	Distance Traveled (km)
PGS13	WTX	22:42:15.10	0.87	3.8
PGS13	SB	22:42:18.60	4.37	20.7
PGS13	CAR	22:42:19.40	5.17	23.3
PGS13	BAR	22:42:20.60	6.37	32.9
PGS14	WTX	20:51:41.80	0.87	3.8
PGS14	SB	20:51:45.20	4.27	20.7
PGS14	CAR	20:51:45.60	4.67	23.3
PGS14	SMC	20:51:46.60	5.67	29.6
PGS14	BAR	20:51:47.20	6.27	32.9
PGS14	BMT	20:51:47.70	6.77	37.7
PGS14	LPM	20:51:48.30	7.37	42.8
PGS15	SMC	18:06:42.10	1.77	4.5
PGS15	WTX	18:06:47.50	7.17	37.5
PGS15	BAR	18:06:51.30	10.97	56.7
PGS15	BMT	18:06:52.00	11.67	63.8
PGS15	LPM	18:06:53.60	13.27	72.5
PGS16	SMC	00:14:24.00	1.77	4.5
PGS16	SB	00:14:28.40	6.17	30.6
PGS16	WTX	00:14:29.30	7.07	37.5
PGS16	BAR	00:14:32.90	10.67	56.7
PGS16	LPM	00:14:35.20	12.97	72.5
PGS17	SMC	00:05:24.70	1.77	4.5
PGS17	BAR	00:05:33.60	10.67	56.7
PGS17	CAR	00:05:30.10	7.17	34.8
PGS17	WTX	00:05:30.10	7.17	37.5
PGS17	BMT	00:05:34.60	11.67	63.8
PGS17	SB	00:05:29.40	6.47	30.6
PGS18	SMC	23:46:46.90	1.77	4.5
PGS18	SB	23:46:51.40	6.27	30.6
PGS18	CAR	23:46:52.00	6.87	34.8
PGS18	WTX	23:46:52.00	6.87	37.5
PGS18	BAR	23:46:56.00	10.87	56.7
PGS18	BMT	23:46:57.66	12.53	63.8
PGS18	LAZ	23:46:59.36	14.23	74.6
PGS19	SMC	23:41:28.84	1.77	4.5
PGS19	SB	23:41:33.40	6.33	30.6
PGS19	CAR	23:41:33.90	6.83	34.8
PGS19	WTX	23:41:34.34	7.27	37.5
PGS19	BAR	23:41:37.90	10.83	56.7
PGS19	BMT	23:41:38.80	11.73	63.8
PGS20	SMC	23:48:26.40	1.77	4.5
PGS20	SB	23:48:31.00	6.37	30.6
PGS20	CAR	23:48:31.50	6.87	34.8
PGS20	LPM	23:48:37.50	12.87	72.5
PGS20	LAZ	23:48:38.00	13.37	74.6
PGS20	BMT	23:48:36.30	11.67	63.8
PGS20	WTX	23:48:31.70	7.07	37.5
PGS21	SNM	18:51:21.35	1.02	3.7
PGS21	WTX	18:51:21.20	0.87	3.8
PGS21	SMC	18:51:25.95	5.62	29.6
PGS21	BAR	18:51:26.50	6.17	32.9
PGS21	BMT	18:51:27.20	6.87	37.7
PGS21	LPM	18:51:27.85	7.52	42.8

TABLE B

Pg READINGS FROM DISTANT SHOTS

Event	Station	Arrival-Time (hour:min:sec)	Travel-Time (sec)	Distance Traveled (km)
PGF1	CM	17:00:15.05	15.05	83.9
PGF1	WTX	17:00:16.71	16.71	93.9
PGF1	SC	17:00:17.16	17.16	97.0
PGF1	CC	17:00:17.84	17.84	102.3
PGF2	LPM	14:00:13.50	13.00	70.5
PGF2	LAD	14:00:18.20	17.70	98.7
PGF2	DM	14:00:11.07	10.57	54.4
PGF2	IC	14:00:11.35	10.85	55.8
PGF2	WTX	14:00:11.80	11.30	58.7
PGF2	SC	14:00:12.87	12.37	64.2
PGF3	CC	23:32:03.85	20.05	113.7
PGF3	WTX	23:32:05.41	21.61	122.2
PGF3	IC	23:32:06.70	22.90	129.7
PGF3	DM	23:32:05.40	21.60	123.6
PGF3	SC	23:32:06.15	22.35	125.2
PGF3	LPM	23:32:03.40	19.60	113.1
PGF4	LAD	20:00:12.90	13.17	70.1
PGF4	LPM	20:00:13.05	13.32	72.6
PGF4	DM	20:00:17.13	17.40	97.0
PGF4	WTX	20:00:18.06	18.33	104.2
PGF4	GM	20:00:19.01	19.28	108.8
PGF5	CC	22:29:35.33	19.68	113.7
PGF5	GM	22:29:34.67	19.02	108.1
PGF5	BG	22:29:35.55	19.90	113.2
PGF5	LPM	22:29:34.65	19.00	113.1
PGF5	LAD	22:29:29.75	14.10	79.4
PGF6	CC	19:57:43.80	19.65	113.7
PGF6	GM	19:57:43.15	19.00	108.1
PGF6	BG	19:57:44.14	19.99	113.2
PGF6	SC	19:57:46.47	22.32	125.2
PGF6	CM	19:57:47.26	23.11	134.5
PGF6	LPM	19:57:43.65	19.50	113.1
PGF6	LAD	19:57:38.15	14.00	79.4
PGF6	WTX	19:57:45.60	21.45	122.2
PGF7	LAD	16:45:12.60	13.12	70.1
PGF7	LPM	16:45:12.80	13.32	72.6
PGF8	LPM	12:35:52.60	13.53	78.1
PGF8	LAD	12:35:57.50	18.43	106.4
PGF8	SNM	12:35:51.20	12.13	66.0
PGF8	CC	12:35:52.60	13.53	74.5
PGF8	GM	12:35:55.30	16.23	91.1
PGF9	SNM	17:00:17.00	17.13	93.3
PGF9	WTX	17:00:17.00	17.13	93.6
PGF9	LPM	17:00:18.40	18.53	106.3
PGF9	LAD	17:00:23.40	23.53	134.7

TABLE C

List Of P* Readings Used

Event	Station	Arrival-Time (hour:min:sec)	Travel-Time (seconds)	Distance Traveled (km)
PS1	NG	18:59:21.10	29.61	184.1
PS1	SC	18:59:20.84	29.35	184.9
PS1	RM	18:59:23.17	31.68	195.2
PS2	SC	18:56:58.18	29.52	182.0
PS2	NG	18:56:57.76	29.10	181.1
PS2	RM	18:56:59.47	30.81	192.3
PS3	NG	19:50:29.26	29.45	185.9
PS3	SC	19:50:29.20	29.39	184.7
PS4	GM	19:11:25.68	29.49	183.1
PS4	SC	19:11:24.49	28.30	181.1
PS4	HC	19:11:24.60	28.41	176.2
PS5	SC	20:18:49.13	28.32	176.6
PS5	GM	20:18:50.18	29.37	183.6
PS5	HC	20:18:48.91	28.10	175.6
PS6	SC	15:45:09.34	18.54	115.5
PS6	IC	15:45:09.40	18.60	117.0
PS6	GM	15:45:07.21	16.41	104.0
PS7	GM	11:59:12.03	21.32	128.5
PS7	SC	11:59:13.74	23.03	147.7
PS7	CC	11:59:14.28	23.57	149.5
PS8	CM	12:17:17.39	25.36	160.2
PS8	CC	12:17:15.80	23.77	149.6
PS8	GM	12:17:12.60	20.57	127.9
PS9	GM	20:44:20.73	23.76	159.7
PS9	CC	20:44:23.12	26.15	178.1
PS9	LAD	20:44:26.55	29.58	196.6
PS10	LAD	05:03:05.15	27.45	171.0
PS10	WTX	05:03:05.85	28.15	176.7
PS11	LPM	10:42:12.05	16.25	100.2
PS11	WTX	10:42:16.10	20.30	128.9
PS12	WTX	21:44:39.70	25.07	161.7
PS12	SB	21:44:37.10	22.47	137.4
PS12	LPM	21:44:45.70	31.07	199.5
PS13	WTX	21:34:28.80	24.37	152.0
PS13	LPM	21:34:33.70	29.27	186.8
PS14	WTX	21:27:12.90	25.06	156.5
PS14	BMT	21:27:15.30	27.46	173.8
PS14	LPM	21:27:17.90	30.06	191.2
PS15	WTX	21:28:28.80	24.07	151.1
PS15	LPM	21:28:33.80	29.07	189.9
PS16	CAR	01:07:06.80	22.46	136.6
PS16	LPM	01:07:12.30	27.96	175.5
PS17	CAR	23:06:02.90	29.07	178.7
PS17	BAR	23:05:59.20	25.37	156.7
PS18	CAR	22:33:46.50	30.96	191.7
PS18	BAR	22:33:42.20	26.66	168.6
PS19	BAR	23:13:55.80	23.97	150.8
PS19	LPM	23:13:52.50	20.67	133.1
PS20	SMC	18:59:22.40	27.77	162.9
PS20	LAZ	18:59:19.40	24.77	143.8
PS21	LPM	20:45:23.10	21.94	130.3
PS21	BAR	20:45:25.30	24.14	148.0

Event	Station	Arrival-Time (hour:min:sec)	Travel-Time (seconds)	Distance Traveled (km)
PS22	LAZ	22:27:59.60	27.91	171.7
PS22	LPM	22:27:52.00	20.31	131.1
PS23	SB	23:52:58.50	30.81	189.5
PS23	CAR	23:52:52.40	24.71	155.5
PS23	SMC	23:52:58.10	30.41	188.0
PS23	LAZ	23:52:54.80	27.11	168.0
PS23	BAR	23:52:48.50	20.81	135.9
PS23	LPM	23:52:47.60	19.91	128.3
PS24	WTX	20:02:27.40	28.97	186.3
PS24	SB	20:02:24.70	26.27	165.1
PS24	CAR	20:02:28.10	29.67	188.8
PS25	WTX	20:22:01.70	30.42	195.0
PS25	SB	20:21:59.30	28.02	173.5
PS25	CAR	20:22:02.50	31.22	198.3
PS25	BMT	20:22:02.80	31.52	198.1
PS26	CAR	00:01:36.90	28.42	172.0
PS26	BAR	00:01:32.20	23.72	148.8

TABLE D

List Of Pn Readings Used

Event	Station	Arrival-Time (hour:min:sec)	Travel-Time (seconds)	Distance Traveled (km)
PN1	DM	08:05:01.55	33.09	220.5
PN1	SC	08:04:58.61	30.15	193.1
PN1	CC	08:05:01.05	32.59	210.4
PN1	WTX	08:05:00.37	31.91	207.9
PN1	TA	08:05:01.22	32.76	219.2
PN2	CC	08:45:40.68	39.13	270.0
PN2	CM	08:45:41.30	39.75	276.5
PN2	TA	08:45:43.30	41.75	290.6
PN2	DM	08:45:42.84	41.29	286.4
PN3	SC	00:06:08.29	70.19	501.6
PN3	WTX	00:06:09.62	71.52	513.5
PN3	CC	00:06:09.12	71.02	509.2
PN3	DM	00:06:11.28	73.18	525.5
PN3	LPM	00:06:13.02	74.92	538.7
PN3	LAD	00:06:08.29	70.19	500.4
PN4	WTX	14:17:02.55	122.45	916.1
PN4	DM	14:17:03.77	123.67	926.0
PN4	TA	14:17:04.53	124.43	931.4
PN4	CM	14:17:03.30	123.20	921.1
PN5	WTX	22:32:13.70	38.26	254.4
PN5	SC	22:32:11.93	36.49	239.7
PN6	GM	13:31:25.15	91.85	664.5
PN6	SC	13:31:27.34	94.04	684.3
PN7	WTX	13:10:05.02	57.62	400.5
PN7	LPM	13:10:09.65	62.25	438.2
PN7	GM	13:10:04.53	57.13	393.8
PN7	DM	13:10:06.13	58.73	410.8
PN7	SC	13:10:03.76	56.36	387.6
PN8	CC	07:41:23.69	34.20	231.1
PN8	CM	07:41:25.50	36.01	248.4
PN9	GM	14:03:37.59	37.09	230.3
PN9	CC	14:03:39.58	39.08	247.0
PN10	LPM	07:57:48.13	101.63	766.0
PN10	LAD	07:57:44.04	97.54	736.1
PN10	WTX	07:57:49.36	102.86	778.8
PN11	LPM	13:00:40.89	38.19	233.7
PN11	LAD	13:00:40.10	37.40	227.1
PN12	LAD	22:54:52.07	40.49	291.0
PN12	LPM	22:54:53.55	41.97	300.5
PN13	LPM	10:56:16.15	43.83	312.1
PN13	LAD	10:56:14.75	42.43	300.5
PN14	LAD	01:39:03.38	43.16	302.3
PN14	LPM	01:39:04.71	44.49	313.1
PN15	LAD	23:28:55.55	42.47	298.5
PN15	LPM	23:28:57.04	43.96	309.6
PN16	WTX	23:51:19.16	117.86	899.1
PN16	BMT	23:51:16.07	114.77	871.0
PN16	LPM	23:51:23.21	121.91	928.6
PN17	BMT	14:16:58.70	118.70	884.5
PN17	WTX	14:17:03.10	123.10	920.2
PN17	SB	14:17:01.80	121.80	905.4

Event	Station	Arrival-Time (hour:min:sec)	Travel-Time (seconds)	Distance Traveled (km)
PN18	BMT	18:04:21.23	117.66	902.1
PN18	WTX	18:04:20.73	117.16	900.2
PN18	LPM	18:04:25.90	122.33	938.3
PN19	LPM	22:32:36.69	42.87	297.2
PN19	BAR	22:32:35.61	41.79	289.9
PN19	WTX	22:32:32.04	38.22	259.9
PN20	SB	20:15:34.09	57.03	400.6
PN20	CAR	20:15:36.98	59.92	432.0
PN20	LPM	20:15:34.96	57.90	413.5
PN20	BAR	20:15:36.64	59.58	425.5
PN20	BMT	20:15:29.58	52.52	372.0
PN20	WTX	20:15:34.76	57.70	408.5
PN21	BMT	12:13:59.76	37.36	260.0
PN21	SMC	12:13:56.66	34.26	234.4
PN22	CAR	17:54:45.77	34.20	237.0
PN22	BAR	17:54:45.13	33.56	232.0
PN22	SMC	17:54:44.75	33.18	231.5
PN22	LPM	17:54:43.73	32.16	221.5
PN22	WTX	17:54:42.53	30.96	213.5
PN23	CAR	11:58:10.55	38.47	264.0
PN23	BMT	11:58:09.93	37.85	261.0
PN24	LPM	00:54:26.61	56.39	420.7
PN24	BMT	00:54:20.81	50.59	378.8
PN25	SMC	02:38:11.08	81.89	570.9
PN25	LPM	02:38:06.08	76.89	541.8
PN25	BMT	02:38:13.08	83.89	598.1
PN25	CAR	02:38:07.54	78.35	546.0
PN26	BMT	20:51:08.68	42.47	283.7
PN26	SB	20:51:12.93	46.72	317.6
PN27	BAR	02:12:59.76	41.23	270.1
PN27	CAR	02:13:02.90	44.37	292.6

Appendix B

Program used to calculate velocity and time-terms

```
C
C     THIS ROUTINE USES THE METHOD OF STRAIGHTFOREWARD MULTIPLE REGRESSION
C     TO SOLVE FOR THE TIME TERMS AND REFRACTOR VELOCITY.  SEE DRAPER AND
C     SMITH FOR  THE MULTIPLE LINEAR REGRESSION TECHNIQUES, AND
C     MURDOCK AND JACKSHA FOR APPLICATION OF THIS TECHNIQUE TO THE TIME
C     TERM PROBLEM.  THE MATRIX INVERSION ROUTINE IS FROM THE USGS LIBRARY IN
C     MENLO PARK (OFFICE OF EARTHQUAKE STUDIES).
C     THE MLR APPROACH ALLOWS SOLVING FOR THE FORMAL UNCERTAINTIES, BASED ON THE
C     ASSUMPTIONS THAT THE PHYSICAL AND STATISTICAL MODELS ARE REALISTIC.
C     (NO SUCH UNCERTAINTIES ARE OUTPUT FROM THE METHOC OF BERRY AND WEST,
C     THEY MAKE INFORMAL ESTIMATES OF THE UNCERTAINTIES OF THE TIME TERMS ONLY
C     --THEY DO NOT ESTIMATE THE UNCERTAINTY OF THE REFRACTOR VELOCITY).
C
C
C     THIS PROGRAM IS SET UP TO HANDLE DATA FOR 80 SITES.  THE NUMBER
C     CAN BE CHANGED BY ALTERRING THE FIRST THREE CARDS OF THE FOLLOW-
C     ING DIMENSION STATEMENT AND THE STATEMENT MA=80 ABOUT  30
C     LINES BELOW, AND THE DIMENSION STATEMENT OF SUBROUTINE MATINV.
C
      DIMENSION SITENM(290),STPTS(290),SGT(290),IP(290)
      DIMENSION IN(290,2),PI(290),Y(290)
      DIMENSION X(95,95),T(95,95),C(95,95)
      DIMENSION RESID(95,95),B(290),TITLE(20)
      DIMENSION ARRAY(290,95),CINV(95,95),XB(290)
      DOUBLE PRECISION CINV,DET,PI,DABS,C,XB,ARRAY,Y
      DOUBLE PRECISION TEMRES,REG,XMAS,RES,SSQ,RESS
      INTEGER STPTS,OUT1
      REAL FILEN*8,OUT*8,DECIDE*8
      REAL  MRESID, IDI, IDJ, ID
C
C     READ IN PARAMETER CARD (INFLOW,OUT1).
C     INFLOW CONTROLS THE FLOW OF THE PROGRAM.  IF IT IS >2 THE PROGRAM
C     STOPS, IF IT=1 THE PROGRAM, DOES ANOTHER SOLUTION ON THE SAME
C     DATA SET, PRESUMABLY WITH ANOTHER VELOCITY CONDITION, AND
C     IF IT=0 THE PROGRAM REALS A DATA SET
C     OUT1, CONTROL THE LEVEL OF OUTPUT: =0 ALLOWED, > 0 SUPPRESSED.
C
C       OUT1 - LISTING OF INPUT DATA,
C
        OPEN(UNIT=25,DEVICE='DSK',ACCESS='SEQIN',FILE='DECIDE.DAT')
        READ(25,997)FILEN
        READ(25,997)OUT
 997    FORMAT(A10)
        OPEN(UNIT=7,DEVICE='DSK',MODE='ASCII',ACCESS='SEQIN',FILE=FILEN)
        OPEN(UNIT=6,DEVICE='DSK',MODE='ASCII',ACCESS='SEQOUT',FILE=OUT)
        OPEN(UNIT=15,DEVICE='DSK',ACCESS='SEQIN',FILE='COMAND.DAT')
      REWIND 15
      REWIND 6
      REWIND 7
      READ (15, 49) TITLE
   49 FORMAT (2X, 20A4 )
   77 CONTINUE
      READ(15,38)INFLOW,OUT1
   38 FORMAT(2X,I2,10X,I2)
C     PROCESS UP TO 1000 CARDS
C
 1021 IF(INFLOW.GT.2)GOTO1090
C
C     ZERO-OUT MATRICES.
C
C
      MA=95
      DO 65 I=1,MA
      SITENM(I)=0.
```

```
      DO 64 J=1,MA
      X(I,J)=0.0
      T(I,J)=0.0
   64 C(I,J)=0.0
   65 CONTINUE
C
C     READ AND PRINT OUT INPUT DATA, CONSTRUCT SITE NAME LIST AND ARRAYS
C
      IF(OUT1.GT.0)GOTO 82
   81 FORMAT (1H1, 5X, 20A4 )
      WRITE (6, 81 ) TITLE
      WRITE (6,66)
   66 FORMAT (//, 5X, 10HINPUT DATA)
      WRITE(6,147)
  147 FORMAT(/,16X,4HDIST,6X,4HTIME,/)
   82 READ(7,1001) IDI,IDJ,XIJ,TIJ
 1001 FORMAT(A4,5X,A4,6X,2F10.3)
      IF(OUT1.GT.0)GOTO 83
      WRITE(6,148) IDI,IDJ,XIJ,TIJ
  148 FORMAT(1X,A4,1X,A4,2F10.2)
   83 SITENM(1) = IDI
      SITENM(2) = IDJ
      X(1,2) = XIJ
      T(1,2) = TIJ
      C(1,2) = 1.0
      KOUNT = 2
      NDATA=1
    2 READ(7,1001,END=1)IDI,IDJ,XIJ,TIJ
      IF (IDI.EQ.IDJ)  GO TO 23
      NDATA=NDATA+1
      IF(OUT1.GT.0)GOTO 19
      WRITE(6,148) IDI,IDJ,XIJ,TIJ
   19 NVAR=0
      ID = IDI
   18 DO 5  K=1,KOUNT
      IF (ID  .EQ. SITENM(K)) GO TO 15
    5 CONTINUE
      GO TO 16
   15 IF(NVAR .EQ. 3)  GO TO 17
      ISUB = K
      NVAR = 3
      ID = IDJ
      GO TO 18
   17 JSUB=K
      GO TO 20
   16 KOUNT = KOUNT + 1
      IF (NVAR .EQ. 3)  GO TO 21
      ISUB= KOUNT
      NVAR = 3
      ID = IDJ
      GO TO 18
   21 JSUB = KOUNT
   20 C(ISUB, JSUB) = 1.0
      X(ISUB,JSUB) = XIJ
      T(ISUB,JSUB) = TIJ
      SITENM(ISUB) = IDI
      SITENM(JSUB) = IDJ
      GO TO 2
    1 CONTINUE
   23 CONTINUE
C
C     PRINT NUMBER OF SITES
C
      IF (KOUNT.LT.MA) GO TO 233
```

```
      WRITE (6,232)
  232 FORMAT (/,41H NUMBER OF SITES EXCEEDS ARRAY DIMENSIONS)
      STOP
C
C
  233 CONTINUE
      KOUNT2=KOUNT+1
C
      DO 230 I=1,NDATA
      DO 231 J=1,KOUNT2
      ARRAY(I,J)=0.0
  231 CONTINUE
  230 CONTINUE
      K=0
      DO 250 I=1,KOUNT
      DO 260 J=1,KOUNT
      IF(T(I,J).EQ.0) GO TO 260
      C(I,J)=1.0
      K=K+1
      ARRAY(K,J)=1.0
      ARRAY(K,I)=1.0
      ARRAY(K,KOUNT2)=X(I,J)
      Y(K)=T(I,J)
  260 CONTINUE
  250 CONTINUE
C
      WRITE(6,990)
  990 FORMAT(1H1)
      WRITE(6,1100)(SITENM(I),I=1,KOUNT)
      DO 270 I=1,NDATA
      WRITE(6,1000)(ARRAY(I,J),J=1,KOUNT2)
  270 CONTINUE
 1000 FORMAT(1X,32(F4.0),F7.2)
      WRITE(6,1100)(SITENM(I),I=1,KOUNT)
 1100 FORMAT(1X,32(A4))
      DO 3000 I=1,KOUNT2
      DO 3000 K=1,I
      C(K,I)=0.
C
C      X NQ. X OF DRAPER AND SMITH
C
      DO 2000 J=1,NDATA
 2000 C(K,I)=C(K,I)+ARRAY(J,K)*ARRAY(J,I)
 3000 C(I,K)=C(K,I)
      DO 100 I=1,KOUNT2
      DO 100 J=1,KOUNT2
  100 CINV(I,J)=C(I,J)
      CALL MATINV(CINV,KOUNT2,DET,IP,IN,PI)
      DO 4000 K=1,KOUNT2
      XB(K)=0.
      DO 4000 J=1,NDATA
C
C     X NQ.Y OF DRAPER AND SMITH
C
 4000 XB(K)=XB(K)+ARRAY(J,K)*Y(J)
      DO 5000 K=1,KOUNT2
      B(K)=0.
      DO 4500 J=1,KOUNT2
C
C     B=(X NQ. X)-1X NQ. Y OF DRAPER AND SMITH
C
 4500 B(K)=B(K)+CINV(K,J)*XB(J)
 5000 CONTINUE
      XDATA=NDATA
```

```
      XDEN2=KOUNT2
      REG=0.
      DO 7000 J=1,KOUNT2
      REG=B(J)*XB(J)+REG
 7000 CONTINUE
      TEMRES=0.0
      DO 7221 J=1,NDATA
      TEMRES=TEMRES+Y(J)*Y(J)
 7221 CONTINUE
      GOTO 1092
 8000 CONTINUE
      RESS=TEMRES-REG
      XMS=SSQ/(XDATA-XDEN2)
      SDS=SQRT(ABS(XMS))
      DO 9000 J=1,NDATA
      YBAR=YBAR+Y(J)
9000  CONTINUE
      YBAR=YBAR/XDATA
      YBARSQ=YBAR*YBAR
      RSQ=(REG-XDATA*YBARSQ)/(TEMRES-XDATA*YBARSQ)
      WRITE(6,1520)
1520  FORMAT(///,'   ANALYSIS OF VARIANCE',///)
      WRITE(6,1521)
1521  FORMAT('    SOURCE SUM OF SQ DEG FREEDOM MEANSQ')
      WRITE(6,1525) REG,KOUNT2
1525  FORMAT('    REGRESSION',E12.4,5X,I3)
      IDF=NDATA-KOUNT2
      WRITE(6,1526) RESS,IDF,XMS
1526  FORMAT('    RESIDUAL',E12.4,5X,I3,5X,E12.4)
      WRITE(6,1530) RSQ
1530  FORMAT(///,'    R SQUARE IS',E12.4)
      WRITE(6,1495)
 1495 FORMAT(1H1,//,10X,'SITE       T TERM       STD. ERROR')
      DO 6000 J=1,KOUNT
      SSE=CINV(J,J)*XMS
      SE=SQRT(ABS(SSE))
 6000 WRITE(6,1500)SITENM(J),B(J),SE
 1500 FORMAT(10X,A4,3X,2(E12.4,3X))
      VAR1OV=CINV(KOUNT2,KOUNT2)*XMS
      WRITE(6,1505)VELCTY,VAR1OV
1505  FORMAT(//1X,'VELOCITY IS  'E12.4,'   VARIANCE OF 1/V IS  'E12.4)
      TEMP1=SQRT(ABS(VAR1OV))
      VELLO=1./(B(KOUNT2)+TEMP1)
      VELHI=1./(B(KOUNT2)-TEMP1)
      WRITE(6,1506) VELHI,VELLO
 1506 FORMAT(//,1X,'    VELHI IS ', E12.4,'   VELLO IS   ',E12.4)
 1090 CONTINUE
        GOTO 1095
1092    CONTINUE
        VELCTY=1/B(KOUNT2)
        WRITE(6,1605)
1605    FORMAT(//,2X,'SITE I SITE J DELTA(I,J) TIME(I,J) RES(I,J)')
        SSQ=0.0
        DO 9500 ND=1,NDATA
        DO 8500 I=1,KOUNT-1
        IF(ARRAY(ND,I).NE.1)GO TO 8500
        DO 7500 J=I+1,KOUNT
        IF(ARRAY(ND,J).NE.1)GO TO 7500
        CALCT=B(I)+B(J)+ARRAY(ND,KOUNT2)/VELCTY
        RES=Y(ND)-CALCT
        WRITE(6,1610)SITENM(I),SITENM(J),ARRAY(ND,KOUNT2),Y(ND),RES
        SSQ=SSQ+(RES*RES)
7500    CONTINUE
8500    CONTINUE
```

```
9500     CONTINUE
1610     FORMAT(2X,A4,3X,A4,3X,F8.2,3X,F8.2,2X,F8.5)
         GOTO 8000
1095     CLOSE(UNIT=5)
         CLOSE(UNIT=6)
         CLOSE(UNIT=7)
       WRITE(5,1091)
 1091 FORMAT('    DO YOU WANT TO RUN ANOTHER DATA FILE?')
       READ(25,997)DECIDE
       IF(DECIDE.EQ.'YES')GOTO 10
       END

CDIMENSIONS FOR MATINV ARE IPIVOT(N),A(N,N),       INDEX(N,2),PIVOT(N).
C      F1 NBSB MATINV
C      MATRIX INVERSION WITH ACCOMPANYING SOLUTION OF LINEAR EQUATIONS
C
C
       SUBROUTINE MATINV(A,N,    DETERM,IPIVOT,INDEX,PIVOT)
C  N IS THE MAXIMUM VALUE FOR N DEGRE.
       DIMENSION A(95,95),        IPIVOT(95),INDEX(95,2),PIVOT(95)
       DOUBLE PRECISION A, PIVOT,SWAP, DETERM,DABS
       EQUIVALENCE (IROW,JROW), (ICOLUM,JCOLUM), (AMAX, T, SWAP)
C
C      INITIALIZATION
C
    10 DETERM=1.0D0
    15 DO 20 J=1,N
       IPIVOT(J)=0
    20 CONTINUE
    30 DO 550 I=1,N
C
C      SEARCH FOR PIVOT ELEMENT
C
    40 AMAX=0.0
    45 DO 105 J=1,N
    50 IF (IPIVOT(J)-1) 60, 105, 60
    60 DO 100 K=1,N
    70 IF (IPIVOT(K)-1) 80, 100, 740
    80 IF (ABS (AMAX)-DABS(A(J,K)))      85, 100, 100
    85 IROW=J
    90 ICOLUM=K
    95 AMAX=A(J,K)
   100 CONTINUE
   105 CONTINUE
   110 IPIVOT(ICOLUM)=IPIVOT(ICOLUM)+1
C
C      INTERCHANGE ROWS TO PUT PIVOT ELEMENT ON DIAGONAL
C
   130 IF (IROW-ICOLUM) 140, 260, 140
   140 DETERM=-DETERM
   150 DO 200 L=1,N
   160 SWAP=A(IROW,L)
   170 A(IROW,L)=A(ICOLUM,L)
   200 A(ICOLUM,L)=SWAP
   260 INDEX(I,1)=IROW
   270 INDEX(I,2)=ICOLUM
   310 PIVOT(I)=A(ICOLUM,ICOLUM)
   312 IF(PIVOT(I).EQ.0.0) GO TO 760
   320 DETERM=DETERM*PIVOT(I)
C
C      DIVIDE PIVOT ROW BY PIVOT ELEMENT
C
   330 A(ICOLUM,ICOLUM)=1.0
   340 DO 350 L=1,N
```

```
350 A(ICOLUM,L)=A(ICOLUM,L)/PIVOT(I)

    REDUCE NON-PIVOT ROWS

380 DO 550 L1=1,N
390 IF(L1-ICOLUM) 400, 550, 400
400 T=A(L1,ICOLUM)
420 A(L1,ICOLUM)=0.0
430 DO 450 L=1,N
450 A(L1,L)=A(L1,L)-A(ICOLUM,L)*T
550 CONTINUE

    INTERCHANGE COLUMNS

600 DO 710 I=1,N
610 L=N+1-I
620 IF (INDEX(L,1)-INDEX(L,2)) 630, 710, 630
630 JROW=INDEX(L,1)
640 JCOLUM=INDEX(L,2)
650 DO 705 K=1,N
660 SWAP=A(K,JROW)
670 A(K,JROW)=A(K,JCOLUM)
700 A(K,JCOLUM)=SWAP
705 CONTINUE
710 CONTINUE
740 RETURN
760 WRITE(6,761)
761 FORMAT(112H * PROGRAM STOPPED BECAUSE A PIVOT ELEMENT IN THE MATRIT
   *X INVERSION SUBROUTINE IS ZERO. MATRIX C MAY BE SINGULAR.    )
762 STOP
    END
```